

**SEISMIC VELOCITIES and REFLECTION SEQUENCES of
WISCONSINAN GLACIAL DEPOSITS in EMERALD BASIN
(SCOTIAN SHELF)**

Johanna Hoehne

Submitted in Partial Fulfillment of the Requirements
For the Degree of Bachelor of Science, Honours
Department of Earth Sciences
Dalhousie University, Halifax, Nova Scotia
March 2001



Dalhousie University

Department of Earth Sciences

Halifax, Nova Scotia

Canada B3H 3J5

(902) 494-2358

FAX (902) 494-6889

DATE APRIL 30th 2001

AUTHOR JOHANNA HOEHNE

TITLE SEISMIC VELOCITIES AND REFLECTION SEQUENCES OF

WISCONSINAN GLACIAL DEPOSITS IN EMERALD BASIN

(SCOTIAN SHELF)

Degree BSc. Convocation MAY 22nd Year 2001

Permission is herewith granted to Dalhousie University to circulate and to have copied for non-commercial purposes, at its discretion, the above title upon the request of individuals or institutions.

THE AUTHOR RESERVES OTHER PUBLICATION RIGHTS, AND NEITHER THE THESIS NOR EXTENSIVE EXTRACTS FROM IT MAY BE PRINTED OR OTHERWISE REPRODUCED WITHOUT THE AUTHOR'S WRITTEN PERMISSION.

THE AUTHOR ATTESTS THAT PERMISSION HAS BEEN OBTAINED FOR THE USE OF ANY COPYRIGHTED MATERIAL APPEARING IN THIS THESIS (OTHER THAN BRIEF EXCERPTS REQUIRING ONLY PROPER ACKNOWLEDGEMENT IN SCHOLARLY WRITING) AND THAT ALL SUCH USE IS CLEARLY ACKNOWLEDGED.

ABSTRACT

Emerald Basin is a 2430 km² depression located on the central Scotian Shelf approximately 40 kilometers off the coast of Nova Scotia. Sleeve-gun reflection data collected in 1994 and Ocean Bottom Seismometer data collected in 1995, were analyzed for this project in order to detail the velocity structures and the lithostratigraphic boundaries of the units present in Emerald Basin. Three units were identified based on their acoustic velocities. Namely, the Scotian Shelf Drift (1.9 km/s) the Mesozoic-Cenozoic strata (2.1 km/s) and the Cambro-Ordovician Meguma Group bedrock (6.1 km/s). Previous works were considered in order to establish a more complex velocity model and to have a velocity value for each lithological unit present in the basin. The velocities of the upper sediments namely, the LaHave Clay and Emerald Silt were not determinable from the data set analyzed due to limitations in resolution, therefore, values of 1.44 km/s and 1.46 km/s (determined by Moran et al. 1991) were utilized for the LaHave Clay and Emerald Silt respectively, for the purposes of mapping.

The boundaries and thicknesses of the LaHave Clay, the Emerald Silt and the Scotian Shelf Drift deposit were determined and mapped during this project. On first interpretation it looked as though the high velocity structure (basement) was present exclusively under the moraine, however when previous work was consulted (Louden 1994) it was determined that the Meguma Group bedrock does occur in the basin as well as under the moraine but it is found at a much greater depth within the basin. The resolution and depth penetration limitations in the data did not allow this unit to be seen and therefore, the unit could not be mapped across the area.

The coincidental occurrence of the high velocity strata under the moraine complex led the author to infer that the position of the moraine was a result of this pre-existing basement structure. When the complex history of the Scotian Shelf is considered it becomes a plausible situation. A major fault complex runs across the Scotian Shelf as a result of early rifting. This would explain the shallower existence of the bedrock under the moraine and the deeper existence in the basin. This idea was taken further to conclude that the shape of the basin and the occurrence of its lithological units and glaciogenic features are a result of how the Wisconsinan ice sheet behaved due to the pre-existing shape of the bedrock.

TABLE OF CONTENTS

ABSTRACT.....	i
TABLE OF CONTENTS.....	ii
TABLE OF FIGURES.....	iii
TABLE OF TABLES.....	vii
ACKNOWLEDGEMENTS.....	viii
CHAPTER 1: INTRODUCTION	
1.1 Introduction to Emerald Basin.....	1
1.2 Scope and Objectives of the Thesis.....	3
1.3 Organization of the Thesis.....	5
CHAPTER 2: BACKGROUND GEOLOGY	
2.1 Tectonic Overview of the Development of the Scotian Shelf.....	6
2.2 General Model for the Deglaciation of the Scotian Shelf.....	7
2.3 Lithostratigraphic Units Found within the Emerald Basin Study Area.....	9
2.3.1 Bedrock.....	11
2.3.2 Scotian Shelf Drift.....	12
2.3.3 Emerald Silt Facies A.....	12
2.3.4 Emerald Silt Facies B.....	13
2.3.5 LaHave Clay.....	13
2.4 Previous Work.....	14
2.4.1 Core Data.....	14
2.4.2 Huntec Reflection Data.....	15
2.5 Site Description of the Study Area.....	17
2.5.1 Scotian Shelf End-Moraine Complex.....	17
2.5.2 Relict Iceberg Furrows.....	18
2.5.3 Lift-off Moraines.....	18
2.5.4 Till Tongues.....	19
2.5.5 Pock Marks.....	22
CHAPTER 3: DATA ACQUISITION AND METHODS OF ANALYSIS	
3.1 General Data Types.....	24
3.2 Acquisition Methods of Ocean Bottom Seismometer Data.....	26
3.3 Methods of Analysis of Ocean Bottom Seismometer Data.....	29
3.4 Acquisition Methods of Sleeve-Gun Reflection Data.....	32
3.5 Methods of Analysis of Sleeve-Gun Reflection Data.....	33

CHAPTER 4: RESULTS

4.1 Slope-Intercept Velocity Models.....	36
4.2 Velocity-Gradient Models.....	40
4.3 Sediment Thickness Models.....	45
4.4 Sources of Error.....	48

CHAPTER 5: INTERPRETATION AND CONCLUSIONS

5.1 Velocity Models.....	51
5.2 Thickness Variation Models.....	56
5.3 A Comparison of Thickness Models.....	58
5.4 Implications of Results.....	59
5.5 Conclusions.....	60
5.6 Recommendations for Future Work.....	62

REFERENCES.....	63
-----------------	----

APPENDIX 1: Horizons Digitized From Reflection Profiles.....	66
--	----

TABLE OF FIGURES

- Figure 1.1** Location map of Emerald Basin. Emerald Basin is located approximately 40 km off the coast of Nova Scotia, on the central Scotian Shelf. The thesis study area is indicated by the black rectangle in the northwest corner of the basin. Core sites recovered in 1987 are represented by orange circles. 2
- Figure 1.2** Bathymetry map of the study area. The red lines represent the ship's track during the seismic reflection survey in 1994. The blue lines represent the ship's track during the Ocean Bottom Seismometer experiment of 1995. The black X's locate the position of the OBS recorders during the HU95-031 experiment. Note the iceberg scours carved into the till on the top of the moraine and the pockmarks visible as dark elliptical depressions in the basin. 4
- Figure 2.1** Cross-section of Emerald Basin along the A-A' profile line. Note the stratigraphic arrangements of the lithological units and their relative thicknesses (modified from King and Fader 1986). 10
- Figure 2.2** Huntect Profiles from Emerald Basin. Note the lift-off moraines and the till tongues occurring within the Emerald Silt units (modified from King and Fader 1986). 16
- Figure 2.3** Model for the formation of a till tongue through a transgressive-regressive ice cycle. In frame 1 the ice is in contact with the bedrock. Deposits of glacial till will then buildup between the ice shelf and the bedrock (2). As the ice starts to retreat water will be present between the till and the ice and glaciomarine sediments, such as Emerald Silt Facies A and B will be deposited (3a). The buoyancy line represents the highest point where the till, the ice and the water are all in contact with each other. In frame 3b the ice shelf has transgressed causing the buoyancy line to move. Frame 3c represents regression and ice retreat. In this frame the product of the transgression-regression (till-tongue) is clearly visible. The final frame (4) illustrates the final stages of regression where the ice is no longer in contact with the sediments (modified from King and Fader 1986). 21
- Figure 3.1** Schematic illustration of vertical incidence seismic geometry with receivers towed and wide angle refraction occurring. The wide angle geometry demonstrates raypath bending as a result of velocity gradients in the sediments of the seafloor. 25

- Figure 3.2** Schematic illustration of the components within an Ocean Bottom Seismometer. 26
- Figure 3.3** Schematic illustration of the Ocean Bottom Seismometer experiment. Note the two anchors at the ends of the OBS string. The horizontal length of the string was approximately 75 meters and the experiment took place at an average depth of 200 meters. 27
- Figure 3.4** Schematic illustration of the components of a sleeve-gun 28
- Figure 3.5** Original OBS data recorded from 95-1A, which was deployed in the basin 30
- Figure 3.6** Original OBS data recorded from OBS 95-2A, which was deployed on the moraine 31
- Figure 4.1** Initial velocity model (continuous lines) based on results from the slope intercept calculations, superimposed on the digitized refraction arrays (dots). The x-axis represents distance from the source in kilometers. The y-axis represents the two-way travel times (seconds); the axis has been reduced by a factor of 8 to reduce the slopes, so that the fit can be seen at a larger scale. P_1 represents the direct arrival from the water wave, P_2 represents the second arrival from the 1.9km/s refractor and P_3 represents the refractor with a velocity of 2.1km/s. 38
- Figure 4.2** Initial velocity model (continuous lines) based on results from the slope intercept calculations, superimposed on the digitized refraction arrays (dots). The x-axis represents distance from the source in kilometers. The y-axis represents the two-way travel times in seconds. P_1 represents the direct arrival from the water wave ($v= 1.49$ km/s), P_2 represents the 1.9 km/s refractor, P_3 represents the 6.1 km/s refractor and P_2P represents the initial reflection arrival, which corresponds to the reflection from the seabed interface. 39
- Figure 4.3** Calculated refraction arrays derived from the proposed velocity model, superimposed on the original 95-1A OBS data. 41
- Figure 4.4** Calculated refraction arrivals derived from the proposed velocity model, superimposed on the original 95-2A OBS data. 42
- Figure 4.5** A contoured depth plot of the seabed. Depths range from 170 meters on the moraine down to 210 meters in the basin. 46
- Figure 4.6a** Contoured thickness map of the LaHave Clay unit in Emerald Basin 47

- Figure 4.6b** Contoured thickness map of the Emerald Silt unit in Emerald Basin 47
- Figure 4.6c** Contoured thickness map of the Scotian Shelf Drift, glacial till unit, in Emerald Basin 47
- Figure 4.7** Example profile from the basin to the moraine (exact location shown on small map to the right) illustrating the horizons chosen and the horizons interpreted as multiples. The large arrow indicates the horizon chosen as the Emerald Silt boundary, while the small arrows indicate the horizons interpreted as multiples. 50
- Figure 5.1** Hunttec Profiles from the 1987 core sites 87-003-002 and 87-003-004. The Hunttec reflection data has a higher resolution than the air-gun reflection data which makes the recognition of the shallow Emerald Basin sediments, such as the LaHave clay and the Emerald silt much clearer. 53
- Figure 5.2** Deep seismic profile recorded in 1994 during CFAV QUEST cruise 211. This profile shows evidence that the high velocity refractor, correlated with the Meguma Group basement strata, is present within Emerald Basin. The reflection that has a two-way travel time of 464 ms was determined to represent the Meguma Group basement. Note that the reflector occurs as a couplet. 55

TABLE OF TABLES

Table 4.1 Initial Velocity-Thickness model determined from OBS 95-1A, based on slope-interval results.	37
Table 4.2 Initial Velocity-Thickness model determined from OBS 95-2A, based on slope-interval results	37
Table 4.3 Summary table of the velocities and thicknesses of the lithological units associated with OBS 95-1A, in the basin.	43
Table 4.4 Summary table of the velocities and thicknesses of the lithological units associated with OBS 95-2A, on the moraine	44

ACKNOWLEDGEMENTS

First and foremost, I would like to thank my supervisors, Dr. Keith Loudon and Robert Courtney, for their guidance and patience throughout the year. Secondly, I would like to thank my family, especially my mother who always has encouraging words. Finally, I would like to thank my friends at Dalhousie, who were always around to provide excellent help and support.

CHAPTER 1

INTRODUCTION

1.1 Introduction to Emerald Basin

Emerald Basin is located approximately 40 kilometers off the coast of Nova Scotia, on the central Scotian Shelf. The basin runs northwest- southeast, approximately parallel to the coast of Nova Scotia. It covers a total area of 2430 km² and has a maximum depth of 290 meters (Sanford et al. 1991) (figure 1.1). The Sambro Moraine, which is part of the Scotian Shelf end-moraine complex, marks the northern boundary of the Emerald Basin. The moraines are arranged in en echelon patterns and are present in water depths of 125 to 175 meters (King 1996). Emerald Basin has been heavily studied in an attempt to gain more information about the last glaciation and the effect that it had on the Maritime region.

The lithological components present in Emerald Basin have been analyzed through core samples and seismic profiles. The lithological units that occur in Emerald Basin were deposited during the last glaciation (Gipp and Piper 1989) and therefore hold many answers about the behaviour and time frame of that event. Sea-level changes of up to -65 meters on the inner Scotian Shelf accompanied the last glacial cycle (Stea et al. 1998). These sea level fluctuations affected the distribution and types of sediments that are found on the Scotian Shelf (Stea et al. 1994). Four distinct units have been mapped in Emerald Basin. The Scotian Shelf drift, a glacial diamicton, was deposited from grounded ice in water depths >120 meters. Emerald Silt facies A and B were formed from subglacial meltout debris from a floating ice shelf. The Holocene LaHave Clay is post-glacial and is confined to the basins and depressions in the shelf (King 1996). A detailed

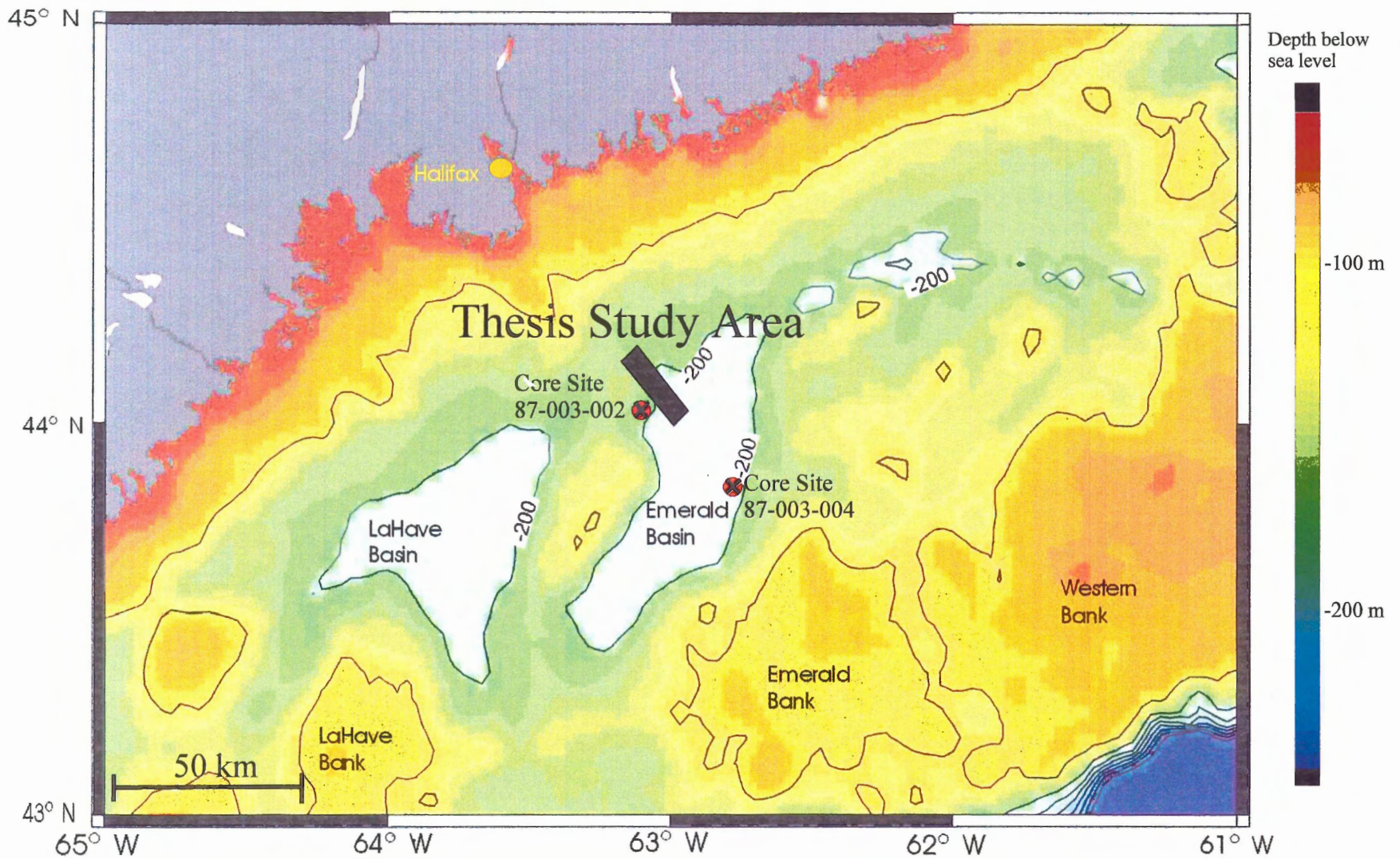


Figure 1.1 Location map of Emerald Basin. Emerald Basin is located approximately 40 km off the coast of Nova Scotia, on the central Scotian Shelf. The thesis study area is indicated by the black rectangle in the northwest corner of the basin. Core sites recovered in 1987 are represented by orange circles.

description of these units, including their ages and lithologies, is given in the geology section of chapter two. Interesting features found in Emerald Basin, in the vicinity of the study area, include iceberg scours, till tongues, end-moraines, lift-off moraines and pockmarks. These features are described in further detail in chapter two.

1.2 Scope and Objectives of the Thesis

The purpose of this project is to derive acoustic velocity relationships using data that were collected by Ocean Bottom Seismometers (OBS) in 1995, to determine the thickness of the lithological layers present in Emerald Basin. OBS recorder 95-1A was deployed at $44^{\circ} 02.34'$ North and $63^{\circ}03.08'$ West which is located in the basin. OBS recorder 95-2A was deployed at $44^{\circ}06.'37.4''$ North and $63^{\circ}06.'22''$ West, on the Sambro Moraine, which is part of the end-moraine complex (figure 1.2). The seismic velocities and thicknesses calculated from the OBS refraction data were used to identify relevant horizons on the reflection profiles. The reflection data, which were analyzed for this thesis, were collected in 1994, with the use of a 40 cu.in. sleeve-gun. These data were used to map the thicknesses and lateral variations of the reflectors and the lithological units that they represent. These maps provide a lithostratigraphy for the units in Emerald Basin, which occur deeper than core samples are able to penetrate.

According to King and Fader (1986) the contact between the Meguma Group rocks and the Mesozoic-Cenozoic strata runs underneath the end-moraine complex. Another goal of this thesis is to see whether it is possible to determine the presence and depth to this boundary from the calculated velocity values from OBS 95-2A. The models produced will promote a better understanding of the environment on the Scotian Shelf

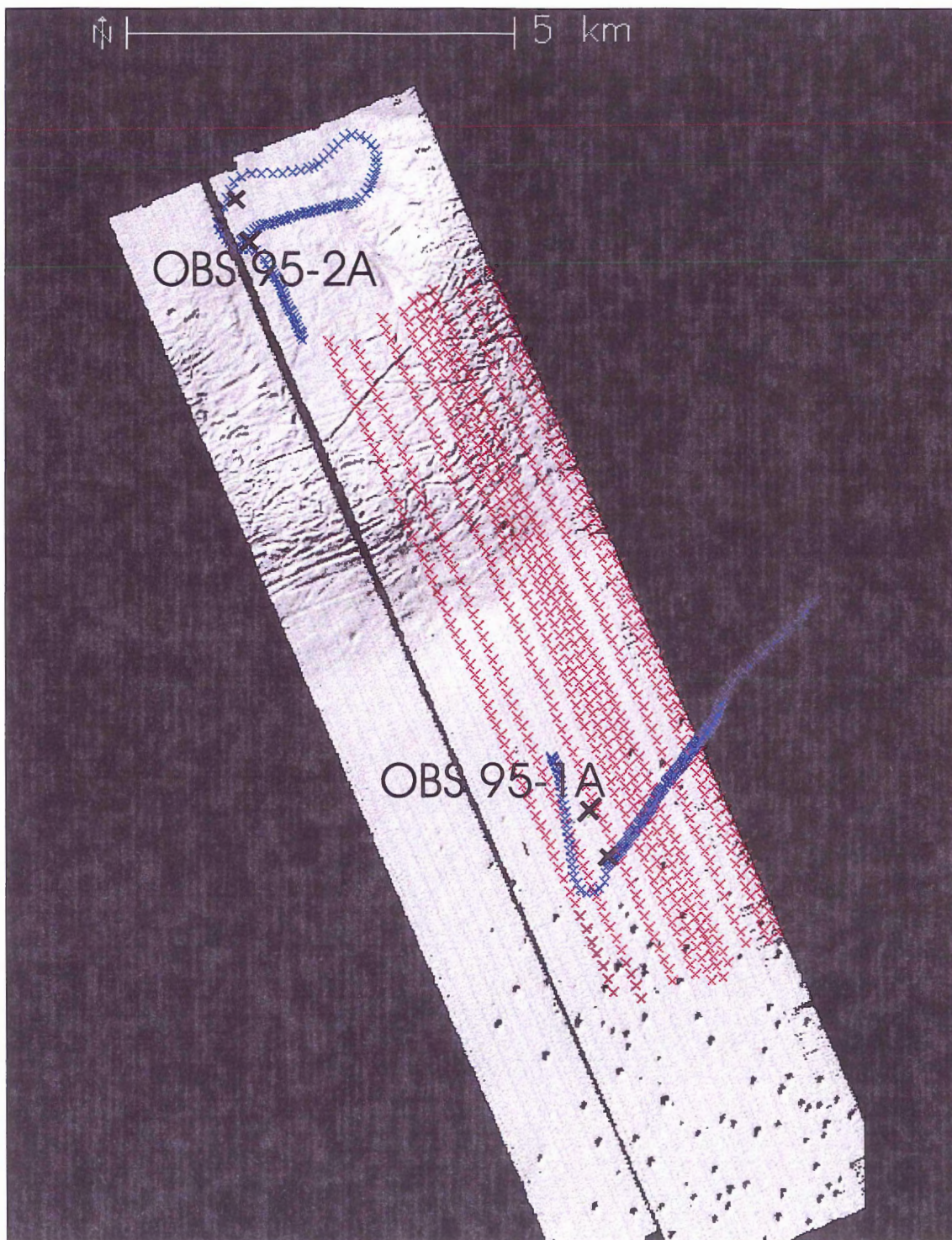


Figure 1.2 Bathymetry map of the study area. The red lines represent the ship's track during the seismic reflection survey in 1994. The blue lines represent the ship's track during the Ocean Bottom Seismometer experiment of 1995. The black X's locate the position of the OBS recorders during the HU95-031 experiment. Note the iceberg scours carved into the till on the top of the moraine and the pockmarks visible as dark elliptical depressions in the basin

during the last glaciation and provide information about the formation of the glaciogenic features found in the study area.

1.3 Organization of the Thesis

Chapter two outlines the tectonic and glacial history of Emerald Basin, and introduces the lithological units and glaciogenic features present in the study area. Chapter three details how the data were collected and analyzed. Chapter four presents the results of the project including the proposed models from the OBS data, and the thickness maps made from the reflection data. Chapter five interprets the results and proposes correlations with previous work as well as summarizes conclusion of the project.

CHAPTER 2

BACKGROUND GEOLOGY

2.1 Tectonic Overview of the Development of the Scotian Shelf

The geological history of offshore eastern Canada can be explained by a cycle of ocean opening and closing. During the Late Precambrian rifting occurred and a Paleozoic passive continental margin bordering the Iapetus Ocean was developed. During the Ordovician the passive margin was subsequently destroyed when the Iapetus closed. This collision continued throughout the Paleozoic and caused subduction and accretion during the development of the Canadian Appalachian Orogen and the Atlantic Margin. The Meguma Group, a Cambro-Ordovician package of marine grey-wackes and shales, forms the easternmost boundary between the Canadian Appalachian Orogen and the Atlantic Margin. The boundaries are steep ductile shears and brittle faults (Keen et al. 1990). The Meguma Group position is relevant to the study area because it provides the basement strata for the area.

The next stage in tectonic development was again one of rifting, this time from within the supercontinent of Pangea (Jansa and Wade 1975). The earliest rifting was between Africa and North America, in the Late Triassic. Narrow, elongate rift basins developed as a result of the rifting (Keen et al. 1990). A major transform fault complex formed southwest of the Grand Banks. This caused the southern portion of the banks to stay with the North American plate, which became a prominent step in the formation of the North American continental margin, and specifically the Scotian Shelf (Jansa and Wade 1975). Continental breakup and seafloor spreading created the present day Atlantic

Ocean. Decoupling of the European and North America plates occurred in the late Jurassic (Jansa and Wade 1975). Once rifting had ceased the area underwent a period of passive subsidence and sedimentation. Thick sequences of both marine and non-marine sediments were deposited from the late Mesozoic through the Cenozoic (Keen et al. 1990). During the analysis of the data for this project, the presence of the African plate (Meguma Group) and the marine and non-marine Mesozoic-Cenozoic strata will be attempted to be determined.

2.2 General Model for the Deglaciation of the Scotian Shelf

The recent development of the Scotian Shelf, including Emerald Basin, can be divided into five stages, which are directly related to the last glaciation. The last glaciation that affected this area occurred from the Wisconsinan to the early Holocene (Amos and Miller 1990).

The beginning of the first stage is marked by the maximum Wisconsinan glacial coverage, which occurred ca. 25 ka (Piper 1991). The maximum coverage extended to the shelf edge and upper continental slope (King 1996). At the beginning of this stage the shelf was covered by a dry-based continental ice sheet. At this time a thin deposit of basal till covered the bedrock (King and Fader 1986). Subglacial deposition was also occurring at the margin of the continental ice sheet at the edge of the continental slope.

Regionally the ice sheet induced an extensive isostatic depression of the crust. In regions of thicker ice, and subsequently greater depression, raised marine features and lowstands were formed at successively higher elevations closer to the ice mass centers (Stea et al. 1994). Towards the end of the first stage, ca. 21 ka (King 2001), glacial retreat

began and as the ice sheet thinned it turned into a wet-based ice shelf and lift-off began in the deeper areas. Glacial erosion is believed to be most effective in a wet-based ice zone (Stea et al. 1994).

The next stage occurred between 20- 16 ka. The ice continued to retreat but remained grounded on the bank areas and on the basin flanks until 15 ka (King 1996). The topographic highs on the shelf acted as anchoring points for the ice rises (Gipp 1994). Deposition of the uppermost part of the blanket till occurred as well as the deposition of the early glaciomarine sediments, such as the Emerald Silt, between the morainic ridges. Recessional sediments were deposited in the basins, while lift-off moraines were forming at the outer boundaries of the basins. Based on core data, lift-off began in central Emerald Basin ca. 18.5 ka (Gipp and Piper 1989). This was also the time of greatest crustal iso-static depression (Quinlan and Beaumont 1982), which is seen by the maximum sea level lowering of -115 meters on the outer shelf (Piper 1991).

Stage three occurred between 16 and 14 ka. when recession reached its maximum and transgression began. Deposition of glaciomarine sediments was continuous during this stage (King and Fader 1986). The re-advances forced marine regression while depositing a distal marine apron and transporting and redistributing sediments (King 2001). The surges and retreats of the ice are thought to have created till tongues along the main moraines and the periphery banks. Till tongues along the northern margin of Emerald Basin have radiocarbon ages of 15,000 to 15,500 C¹⁴ years BP (Stea et al. 1994). A widespread unconformity is registered in the central basins and is the result of a terrestrial re-advance of the glacier. This event triggered strong bottom currents, which caused an influx of ice rifted sandy sediments, such as Emerald Basin Silt facies A, to be

deposited (King 1994). The ice margin must have retreated shortly after the erosional event, because deposition of the Emerald Silt facies A in the northeast of Emerald Basin ended ca. 14.5 ka (King and Fader 1988).

Stage four represents a period of general retreat of ice from the central shelf. This occurred between 14 and 12 ka. Open water conditions developed and the bottom currents had a large influence on the distribution and erosion of the sediments (King and Fader 1986). At this stage pro-glacial sediments, such as Emerald Silt facies B were deposited (King 2001). During this stage of final retreat the crust had rebounded from the glacio-isostatic depression of the ice sheet (King and Fader 1986).

The final stage, which occurred between 12 to 10 ka, records a period of lowest relative sea level (- 65m) for the inner shelf, and subsequent transgression (Stea et al. 1994). During this stage large areas of the shelf were exposed sub-aerially, which left the properties of the sediments open for modification. Across the outer banks large areas of well-sorted gravel were deposited as transgression progressed. In the basins fine-grained sediments such as the LaHave Clay were deposited (Piper 1991).

2.3 Lithostratigraphic Units Found within the Emerald Basin Study Area

The majority of the units within Emerald Basin were deposited during the Wisconsin glacialiation. Emerald Basin consists of three glaciogenic stratigraphic units that lie conformably over the bedrock. These units include the Scotian Shelf Drift, Emerald Silt facies A and B, and the LaHave Clay (King and Fader 1986) (figure 2.1). The units are associated with important phases of glacial history and the boundaries between the lithological units mark major environmental changes (Hall et al. 1998).

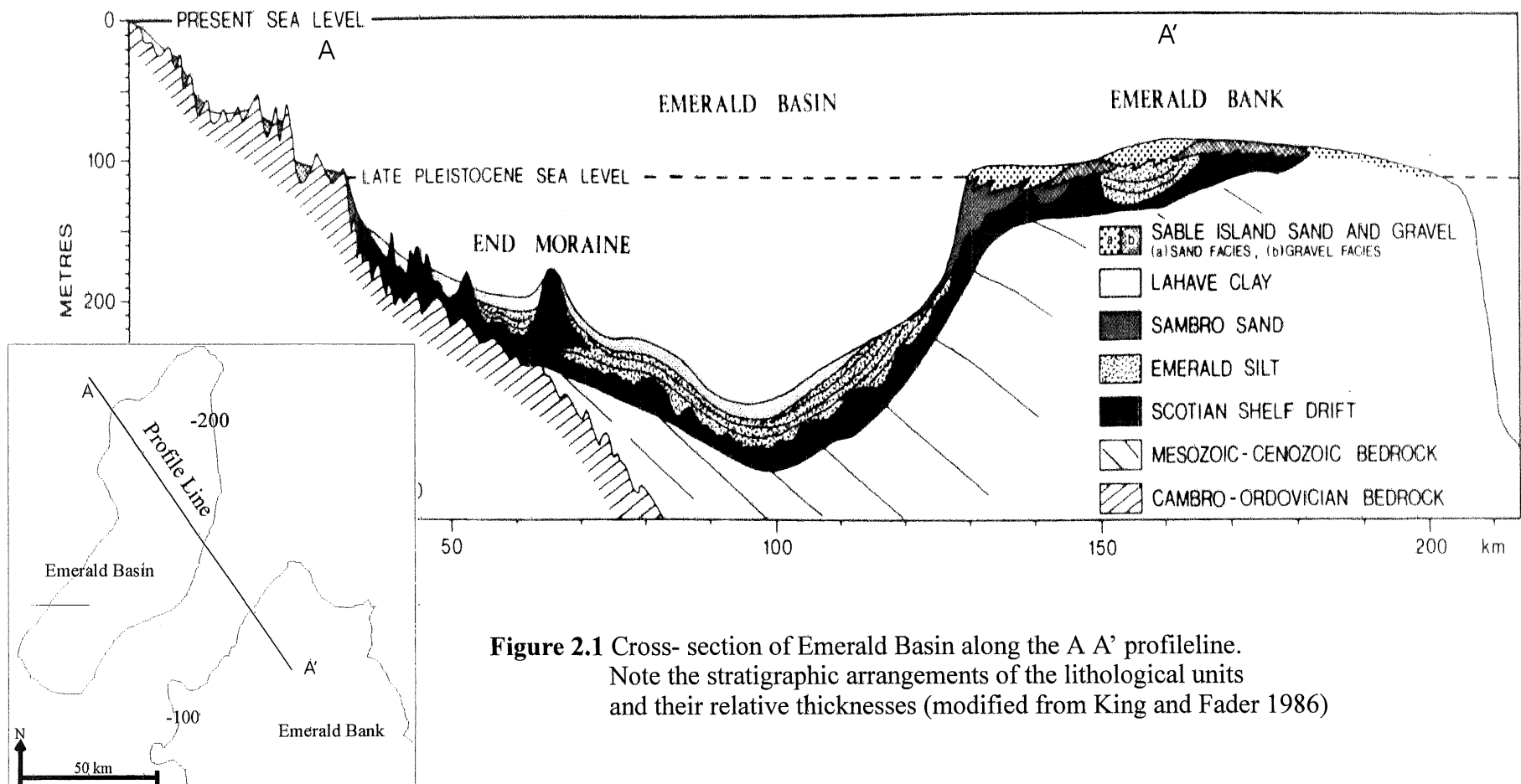


Figure 2.1 Cross-section of Emerald Basin along the A A' profileline. Note the stratigraphic arrangements of the lithological units and their relative thicknesses (modified from King and Fader 1986)

Various associated glacial features also occur in or surrounding Emerald Basin and they will also be discussed in this chapter.

2.3.1 Bedrock

The bedrock underlying the surficial stratigraphic units consists of low-grade Cambro-Ordovician metasedimentary rocks, of the Meguma Group, and a thick prism of accreted Mesozoic-Cenozoic strata associated with the development of the North Atlantic ocean basin (Wade and MacLean 1990). The surface of the bedrock represents a submerged coastal plain that has been physically modified by glacial erosion (King and Fader 1986). The shape of the present bedrock has a great influence on the bathymetry of the shelf and its basins.

Various seismic experiments have been done on the Scotian Shelf to determine the acoustic properties of the bedrock strata. According to Barrett et al. (1964) the crustal Meguma layer has a velocity of 6.10- 6.15 km/s, based on calculated values from compressional waves on seismic refraction profiles. Wade and MacLean (1990) state that the acoustic velocity for the Meguma Group is 5.5 km/s. Brocher (1983) used high-quality refraction profiles, which were collected using tele-metered ocean bottom seismometers (TOBS), to determine that the acoustic velocities for the Pre-Cretaceous strata to be between 5.6 km/s and 6.1 km/s.

2.3.2 The Scotian Shelf Drift

The Scotian Shelf Drift is a glacial till that was deposited, from a grounded ice shelf, during the Pleistocene (Gipp and Piper 1989). It occurs at the base of the other two surficial sequences, conformably overlying the bedrock. It is very dark greyish brown, poorly sorted and cohesive. The Scotian Shelf Drift contains sandy clay and silt with variable gravel. Its thickness can range from 0-100 meters. On a seismic record this unit can be identified by its incoherent reflections, with scattered point source reflections (King and Fader 1986).

2.3.3 Emerald Silt facies A

Emerald Silt facies A was also deposited in the Pleistocene, in a time period equivalent to the Scotian Shelf Drift. This unit is dark greyish brown and poorly sorted. It consists of clayey and sandy silt and some gravel. This unit can range from 0–100 meters in thickness (King and Fader 1986). Emerald Silt facies A is subglacial in origin, and was deposited by subglacial meltout debris from a floating ice shelf. The unit has rhythmic banding due to the differential sorting of material settling through the water column. On a seismic record this unit can be distinguished based on its high amplitude continuous coherent reflections and its highly conformable to substrate irregularities (King and Fader 1986).

2.3.4 Emerald Silt facies B

Emerald Silt facies B was deposited during the Pleistocene and is proglacial in origin. This represents a time of general ice retreat from the central shelf, when periods of open water conditions caused the bottom currents to have a great influence on the distribution of sediments. This resulted in a wide regional unconformity that exists at the base of facies B (King and Fader 1986). The unconformity is best developed on the flanks of the basin. In Emerald Basin, facies B overlies facies A. Emerald Silt facies B consists of darkish greyish brown, poorly sorted clayey to sandy silt with some gravel. Unlike facies A, facies B has poorly developed rhythmic banding. Facies B has a thickness that ranges from 0- 40 meters. On a seismic record Emerald Silt facies B can be recognized by medium to low amplitude continuous coherent reflections, with some degree of ponded sedimentation style (King and Fader 1986).

2.3.5 LaHave Clay

The LaHave Clay is a post-glacial deposit and was deposited during the Holocene. It is greyish brown and grades from soft, silty clay to clayey silt (King and Fader 1986). This unit is confined mainly to the basins and depressions on the Scotian Shelf where it is ponded, as a loosely compacted unit, over the underlying sediments. It is derived from a winnowing of the fine material from glacial sediments on the banks during relative sea level rise, and from the adjacent land areas. On a seismic record the LaHave Clay can be recognized by its generally transparent appearance, with only a few weak continuous coherent reflections showing up at the base of the unit (King and Fader 1986).

2.4 Previous Work in Emerald Basin

2.4.1 Core Data

Long piston core samples were recovered from Emerald Basin in 1987. The location of cores 87-003-02 and 87-003-04 can be seen on figure 1.1. Physical properties such as the thickness and acoustic velocity of the lithological units were determined from these cores. These values will be considered relevant for correlation with the data of this project based on their proximity to the study area.

Core 87-003-02 is 17 meters long (Hall et al. 1998) and recovered LaHave Clay and Emerald Silt. The LaHave Clay unit is 8 meters thick and the Emerald Silt makes up the remaining 9 meters. According to the Hunttec seismic profile that was run across the core site, the core did not penetrate down to the Scotian Shelf drift, making the total thickness of the Emerald Silt unit greater than 9 meters (Moran et al. 1991). The average acoustic velocity for the LaHave Clay is 1.44 km/s, while the average for the Emerald Silt is 1.45 km/s (Moran et al. 1991). These acoustic velocities are lower than the acoustic velocity of water because of the high water content.

Core 87-003-04 is 19 meters long; approximately 5 meters of LaHave clay were recovered and the remainder of the recovered sediment was Emerald Silt (Moran et al. 1991). Again the core did not penetrate down as far as the Scotian Shelf drift so based on the Hunttec seismic profile it is assumed that the Emerald Silt continues deeper than the 14 meters that were recovered. The average acoustic velocities measured from this core are the same as the previous core, with 1.44 km/s representing the LaHave Clay and 1.45 km/s representing the Emerald Silt (Moran et al. 1989). A seismic refraction experiment performed on the Scotian Shelf in 1983 (Brocher 1983) determined velocities in the range

of 1.5 km/s for Pleistocene- Holocene sediments, 2.2 km/s - 3.9 km/s for the Cenozoic sediments, and 5.6 km/s – 6.1 km/s for pre-early Cretaceous strata.

2.4.2 Hunttec Reflection Data

Previous seismic studies have been performed in Emerald Basin, for example HU 87-003 and HU 94-021. The studies that contain information pertinent to this project are the high-resolution Hunttec reflection profiles (figure 2.2). The Hunttec profiler works on a much higher frequency than sleeve-gun reflection surveys. The frequency spectrum for a Hunttec survey generally ranges from 1000 to 6000 Hz, and as a result higher resolution profiles are created. These profiles then display more details of the upper sedimentary units. Since the reflection data considered for this project were collected from a lower frequency sleeve-gun survey, the Hunttec information was incorporated to gain information on the upper sedimentary units in order to build on the complexity and detail of the velocity model.

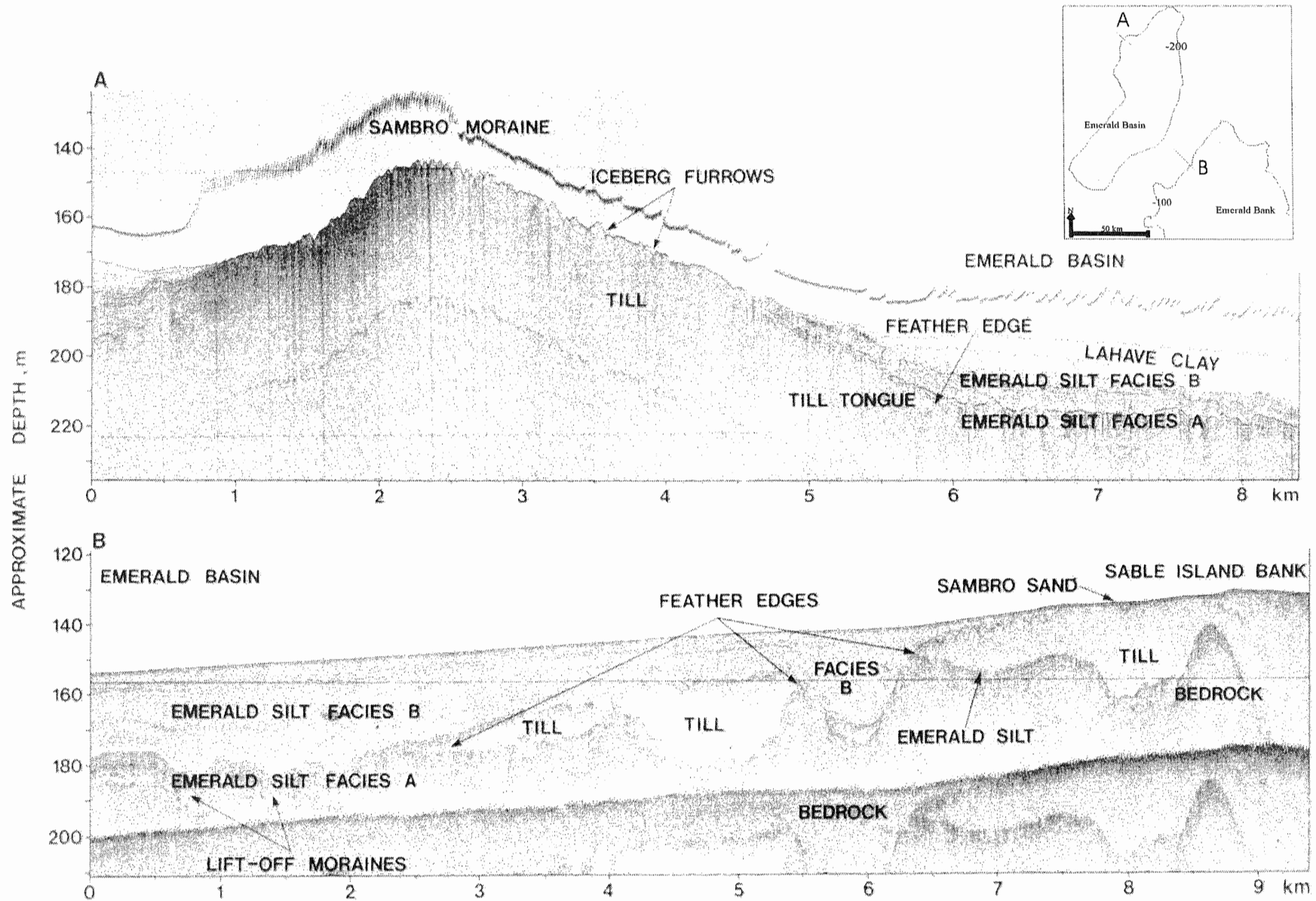


Figure 2.2 Huntect Profiles from Emerald Basin. Note the lift-off moraines and the till tongues occurring within the Emerald Silt units (modified from King and Fader 1986)

2.5 Site Description of the Study Area

Besides the lithological units that comprise Emerald Basin, various process-driven features are also present. These features are glacially controlled, in the case of the End-Moraine Complex, the lift-off moraines, iceberg scours and till- tongues, or organically controlled such as the pockmarks.

2.5.1 Scotian Shelf End-Moraine Complex

The Scotian Shelf End-Moraine Complex was formed at the buoyancy line of the Laurentian ice shelf. The moraines are located at the seaward margin of the inner Scotian Shelf and the Sambro Moraine provides the northern boundary for Emerald Basin (Stea et al. 1998). The end-moraine complex is a series of large sea-bottom ridges, which are located 30-40 kilometers off the coast of Nova Scotia. The end moraine consists dominantly of the Scotian Shelf Drift, a diamicton consisting of massive to stratified, matrix to clast supported, sediments interbedded with mass-flow sands and debris flows (King 1993). The deposits are olive gray, which reflects their derivation from the greenschist facies Meguma Group metasediments (Stea et al. 1998). The end-moraines developed as dominant features during the maximum point of glacial recession and therefore provide evidence for the last major advance of the ice sheet, since they are associated with an area where the ice remained grounded (King and Fader 1986).

2.5.2 Relict Iceberg Furrows

Iceberg furrows are scoured into the surface of the till to depths of 2-3 meters on the moraine belt (figure 1.2). The width of the scours can range up to 200 meters (King and Fader 1986). Iceberg scours are created when grounded icebergs are dragged over the sea-bottom by currents (Benn and Evans 1998). Buried iceberg furrows are also visible on reflection profiles. They are visible in Emerald Silt facies A and B. These scours are 2-5 meters deep, and 30-120 meters wide. Although they look similar to the pockmarks in size, the iceberg scours have raised edges and asymmetrical deposits on their peripheries (Gipp 1994). These features have preferred orientations, which show southwest-northeast trends along the eastern flank and south-north trends along the northeastern flank (Gipp 1993). The direction of ice retreat can be inferred from these trends. Gipp (1994) concluded that the icebergs exited Emerald Basin via an eastern channel. The age of these features is estimated to range from 18 ka to 13 ka, based on radiocarbon dates from shells (Gipp 1998), which also leads to conclusions for the time of ice retreat.

2.5.3 Lift-off Moraines

Lift-off moraines are commonly described as subglacial, recessional features that occur as parallel ridges of till that can be found on the surface of the basal till in the basin areas (Gipp 1993b) (figure 2.2). They have also been interpreted as seasonal end-moraine type deposits (R. Courtney personal communication 2001). Lift-off moraines can be up to 3 meters high and 20-80 meters wide (Gipp 1993b). If they are sub-glacial deposits they developed as the grounded ice shelf lifts off the seabed. Fields of lift-off moraines are remarkably well preserved, which indicates that they were recessional since they would

not be preserved if a glacial advance had affected the area after deposition. If the conformable glaciomarine succession above the moraine is thick, this indicates that the ice remained pinned for an extended period of time after lift-off (King and Fader 1986). This situation is common in the glacially-overdeepened basins of the continental shelf, such as Emerald Basin (Gipp 1993b). Lift-off moraines are commonly associated with Emerald Silt facies A, and according to King and Fader (1986), it is often difficult to define where the upper surface of the moraine ends and where the overlying conformable glaciomarine sediments begin. The flanks of the ridges are very steep, and bands of Emerald Silt can commonly be correlated between them. The correlation between the ridges and the deposits of Emerald Silt suggest that they were probably deposited simultaneously (King and Fader 1986). The moraines are formed in a perpendicular direction to the last ice flow, therefore they can provide more evidence for the direction of ice retreat (Gipp 1993b). The position of the moraines in the Emerald Basin vicinity indicate that the ice retreated northwards towards Nova Scotia but also locally to topographic highs around the basin, which acted as temporary anchoring points around the basin (Gipp 1993b).

2.5.4 Till Tongues

Till tongues are wedge-shaped bodies of till interbedded with Emerald Silt. They are large ice-marginal deposits associated with floating front ice-margins (King 1993). Till tongues can be found within the moraines at the northeastern edge of Emerald Basin (figure 2.2). They are usually confined to the flanks of the depressions or basins on the Scotian Shelf. They are also usually confined to the distal, seaward side of the moraine

complex. Till tongues vary in length from 100 meters to over 25 kilometers. The thickness is also variable from a few meters to over 40 meters. At the thin, or feathered edge of the tongues, continuous coherent reflections of Emerald Silt splay, and continue under or over the edge of the tongues. Under the tongues the Emerald Silt unit usually terminates abruptly against the till, but in some circumstances it may continue under the moraine complex. The relationship between the till tongue and the Emerald Silt varies between the top and the bottom surface of the tongues, the bottom surfaces are generally smoother, and the tongues lie parallel to the underlying Emerald Silt reflections (King and Fader 1986).

According to King and Fader (1986) till tongues indicate a progressive development over a significant period of time. They are formed during the migration of the point of contact between the ice and the seabed, known as the buoyancy line. This migration could be caused by numerous factors including: changes in water depth due to variations in the topography of the seabed, changes in the size and draft of the ice mass itself, climatic conditions, or isostatic or eustatic sea level changes. The creation of a till tongue is demonstrated schematically in figure 2.3. During the time of advance of the buoyancy line the ice would make contact with the seabed by vertical motion. The Scotian Shelf Drift would have been deposited behind the ice and the Emerald Silt would have been deposited in front of the lift-off point. During a complete cycle of transgression and regression of the lift-off point, a wedge of till would have been formed with the glaciomarine Emerald Silt lying under and over it (King and Fader 1986).

Other theories on how till-tongues form also exist. According to Gipp (1994), the till-tongues are formed by gravity-flow processes because they occupy local topographic

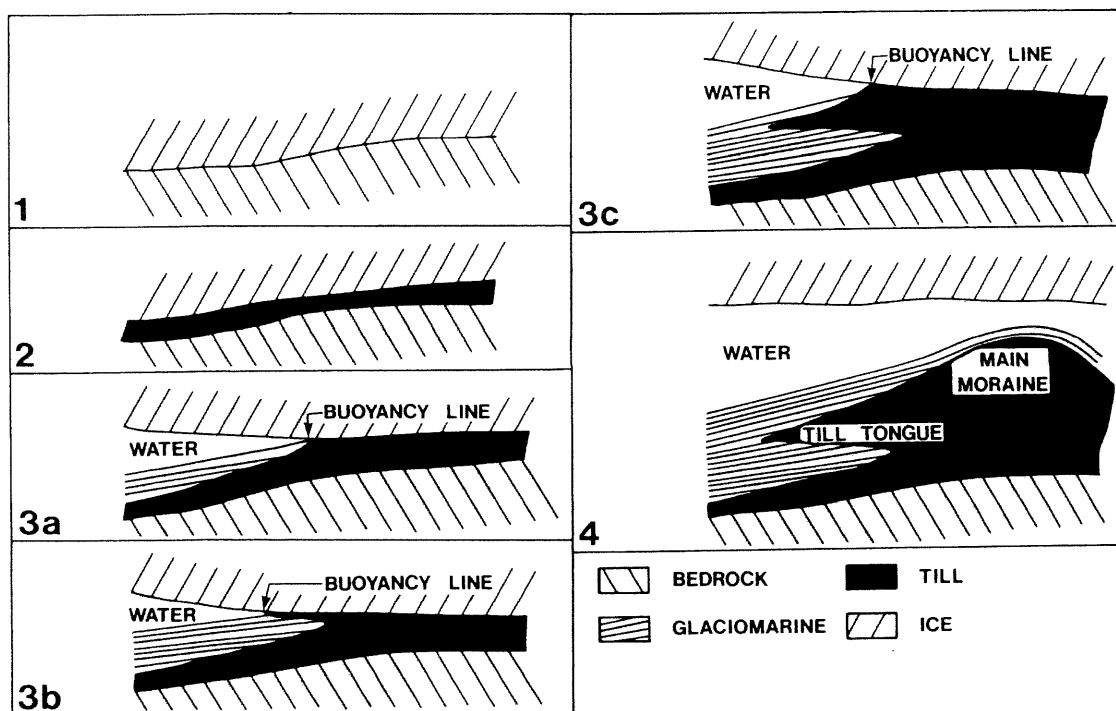


Figure 2.3 Model for the formation of a till tongue through a transgressive-regressive ice cycle. In frame 1 the ice is in contact with the bedrock. Deposits of glacial till will then buildup between the ice shelf and the bedrock (2). As the ice starts to retreat water will be present between the till and the ice and glaciomarine sediments, such as Emerald Silt Facies A and B will be deposited (3a). The buoyancy line represents the highest point where the till, the ice and the water are all in contact with each other. In frame 3b the ice shelf has transgressed causing the buoyancy line to move. Frame 3c represents regression and ice retreat. In this frame the product of the transgression-regression (till-tongue) is clearly visible. The final frame (4) illustrates the final stages of regression where the ice is no longer in contact with the sediments (modified from King and Fader 1986).

flows along gentle slopes. Their morphology and acoustic character resembles those of debris flows, but it is unclear whether they would represent a single event or an accumulation of flow events. In this situation the features would have formed independently from any ice interactions.

2.5.5 Pockmarks

Pockmarks are visible within the basin on the bathymetry map (figure 1.2). They are elliptical, cone-shaped craters on the seabed created by the escape of gas (King and MacLean 1970). The craters are created by a process known as gas-turbation, where significant volumes of sediments are eroded due to the escaping gases (Josenhans et al. 1978). The gases escaping in this case are likely deep bedrock- generated hydrocarbon gases (Fader 1991; Gipp 1994). It is possible that the escaping gases travel along a restricted path from a point source in the bedrock to the top of the sediment without any lateral movement (Vilks and Rashid 1976). In Emerald Basin the gases travel from the underlying Cenozoic and Mesozoic strata up through the silts and clay, and their elliptical shape is a result of the bottom tidal currents reworking the shape of the crater (Josenhans et al. 1978). The eroded craters can range from a few meters to >300 meters in diameter and from <1meter to 30 meters in depth (Fader 1991). The size and distribution of the pockmarks is controlled primarily by the type of sediment in which they occur (Gipp 1994). Large, deep pockmarks occur within the LaHave Clay, where the thickness is greater than 6 meters; while small, shallow pockmarks occur in the LaHave Clay that is less than 6 meters thick (Josenhans et at. 1978). The concentrations of gases found within

the pockmarks in Emerald Basin do not exceed 20ppm, which is a background value (Vilks and Rashid 1976).

CHAPTER 3

DATA ACQUISITION AND METHODS OF ANALYSIS

3.1 General Data Types

Sleeve-gun reflection data and Ocean Bottom Seismometer (OBS) refraction data were both used for the analysis of this project (figure 3.1). During a seismic reflection survey a seismic wave is generated at a source and the transit time from the source to an acoustic boundary and back to the receiver is recorded. This quantity is known as the two-way travel time (twtt). This data is then used to obtain information on the geometry and physical properties of the materials that the seismic wave has travelled through. The twtt (which is in a time domain) can then be converted to depth, using seismic velocities determined by refraction data.

Seismic refraction surveys are based on the principle that when a seismic wave encounters a velocity contrast the direction of the wave will change (refract) as it enters the new medium. The raypaths are refracted according to Snell's Law, which states:

$$\frac{\sin \theta_1}{V_1} = \frac{\sin \theta_2}{V_2}$$

where $\sin \theta_1$ = angle of incidence
 $\sin \theta_2$ = angle of refraction
 V_1 = velocity of medium 1
 V_2 = velocity of medium 2 (refractor)

Seismic velocity changes are related to bulk modulus, rigidity, and density, therefore measuring the refraction and calculating the velocity of a wave can lead to information about the physical properties of the material. The importance of refraction data is that lateral changes in thickness and depth of lithological units can be resolved once the data is

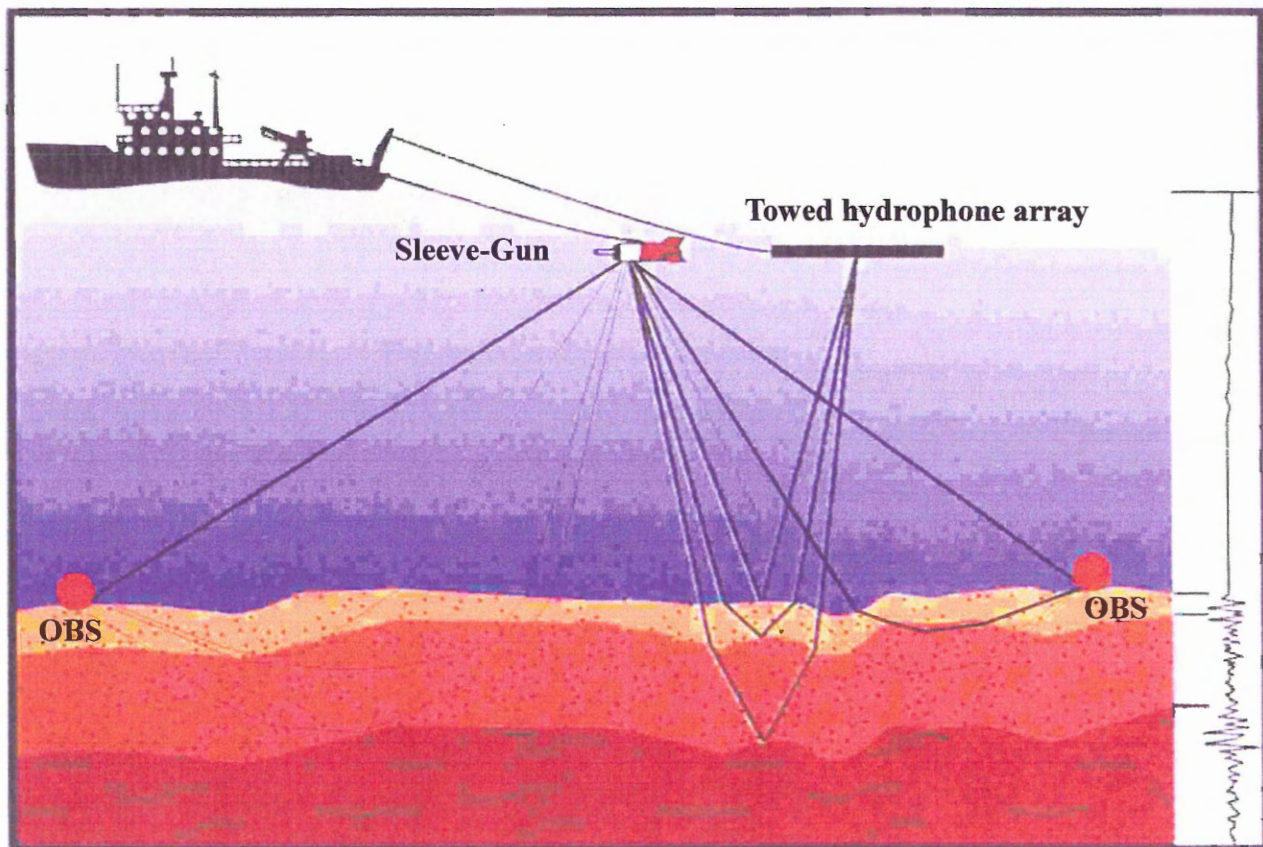


Figure 3.1 Schematic illustration of vertical incidence seismic geometry with receivers towed and wide angle refraction occurring. The wide angle geometry demonstrates raypath bending as a result of velocity gradients in the sediments of the seafloor.

converted to the spatial domain. The data analysed for this project were collected using Ocean Bottom Seismometers (OBS) that were placed on the seafloor.

3.2 Acquisition Methods of Ocean Bottom Seismometer Data

OBS instruments are self-contained seismographs. The main components that make up the devices are: one externally mounted hydrophone and three internally mounted geophones, a 12kHz Pinger, a digital data logger, a clock and a battery pack (figure 3.2).

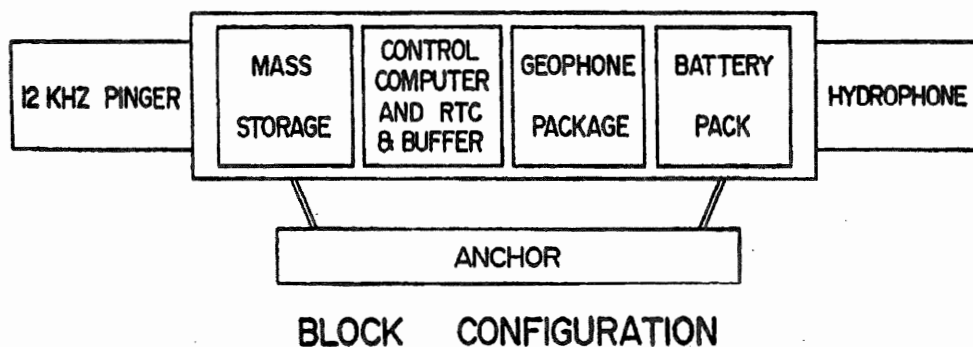


Figure 3.2 Schematic illustration of the components within an Ocean Bottom Seismometer

The OBS data analyzed for this portion of the project were collected in 1995, during Bedford Institute of Oceanography Cruise HUD95-030B. A string of five OBSs (A-E) was deployed in two sites in Emerald Basin (figure 3.3). Buoys were attached to the two ends of the OBS arrays so that the oceanographic ship could locate the OBSs while they were on the bottom. The OBSs were placed on the seabed for a number of reasons, namely so that most of the travel-time through the water would be eliminated, noise would be reduced, and earlier refraction arrivals would be visible. For this project only the data from OBS A were analyzed for each position. In this case OBS 95-1A was deployed at

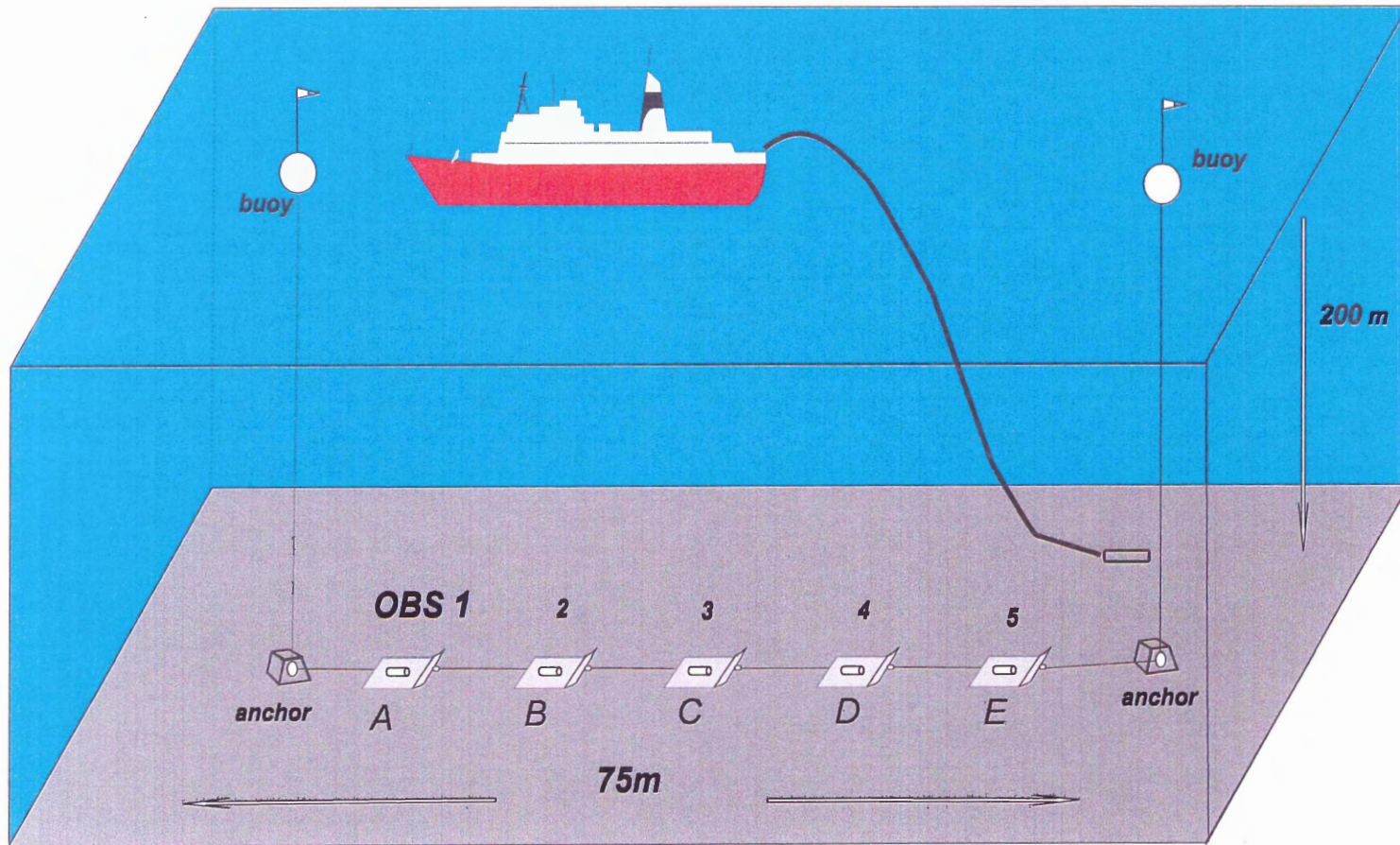


Figure 3.3 Schematic illustration of the Ocean Bottom Seismometer experiment. Note the two anchors at the ends of the OBS string. The horizontal length of the string was approximately 75 meters and the experiment took place at an average depth of 200 meters.

44°02.34' North and 63°03.08' West, which corresponds to an area in the basin. OBS 95-2A was deployed at 44°06'.37.4" North and 63°06'.22" West, which corresponds to an area on the moraine (figure 1.2).

The acoustic source for the OBS experiment was a 40 cu. in. sleeve-gun (figure 3.4). The firing rate was set to 10 seconds. The OBS refraction data are initially stored in 2 Mb RAM, when this RAM is full the contents are transferred to a hard disk. This process takes approximately 10-20 seconds, during which time data acquisition is interrupted. These periodic interruptions are visible as blank spaces at regular intervals across the refraction array. The final data are written to a hard disk once an acoustic release code is transmitted, and the data are transferred to an external Exabyte disk once the OBS has been recovered.

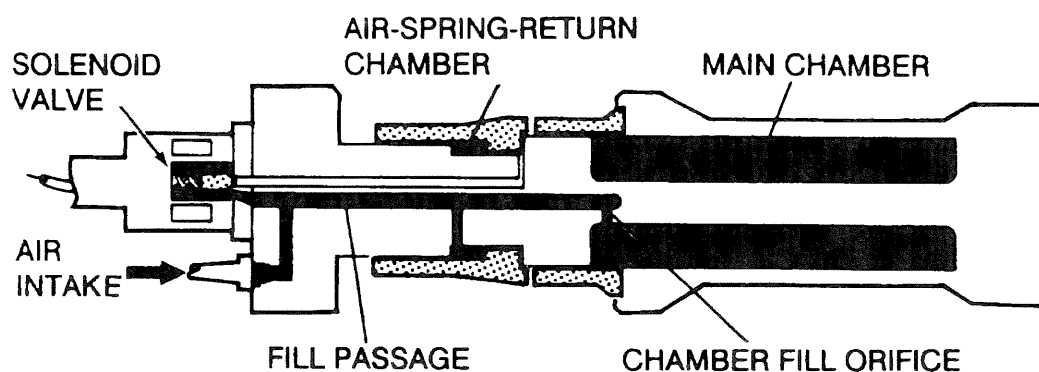


Figure 3.4 Schematic illustration of the components of a sleeve-gun

OBS arrays are displayed as two-way travel time versus horizontal offset. For this project the parameters on the axis were in milliseconds versus meters (figures 3.5, 3.6). Offset (x-axis) is a measure of distance from the source, which was calibrated for these plots using the previously calculated water velocity of 1.49 km/s.

3.3 Methods of Analysis of Ocean Bottom Seismometer Data

OBS refraction data are used to determine the acoustic compressional velocity (p-wave) of the lithological units, through which the raypaths have travelled. This is done by calculating the slopes ($\Delta T/\Delta X$) of the refraction arrivals from the OBS arrays. The slope intercept is used to determine the two-way travel time to each layer.

The initial analysis required the refracted arrivals from the OBS arrays 95-1A and 95-2A to be digitized. The digitized values were then put into an Excel spreadsheet and the velocities and arrival times were calculated (based on the slopes and the y-intercepts). The thicknesses were calculated next by inputting the velocities and arrival times into the following equation:

$$T_j = 2 \cdot \sum_{i=1}^{j-1} d_i (1/V_i^2 - 1/V_j^2)^{1/2}$$

where: T= arrival time,
d = thickness,
V= velocity

The thickness and velocities calculated at each OBS site were then entered as parameters into the computer program (Raytrace). The calculated program results were overlaid onto the original digitized OBS data points to check the accuracy of the calculated model.

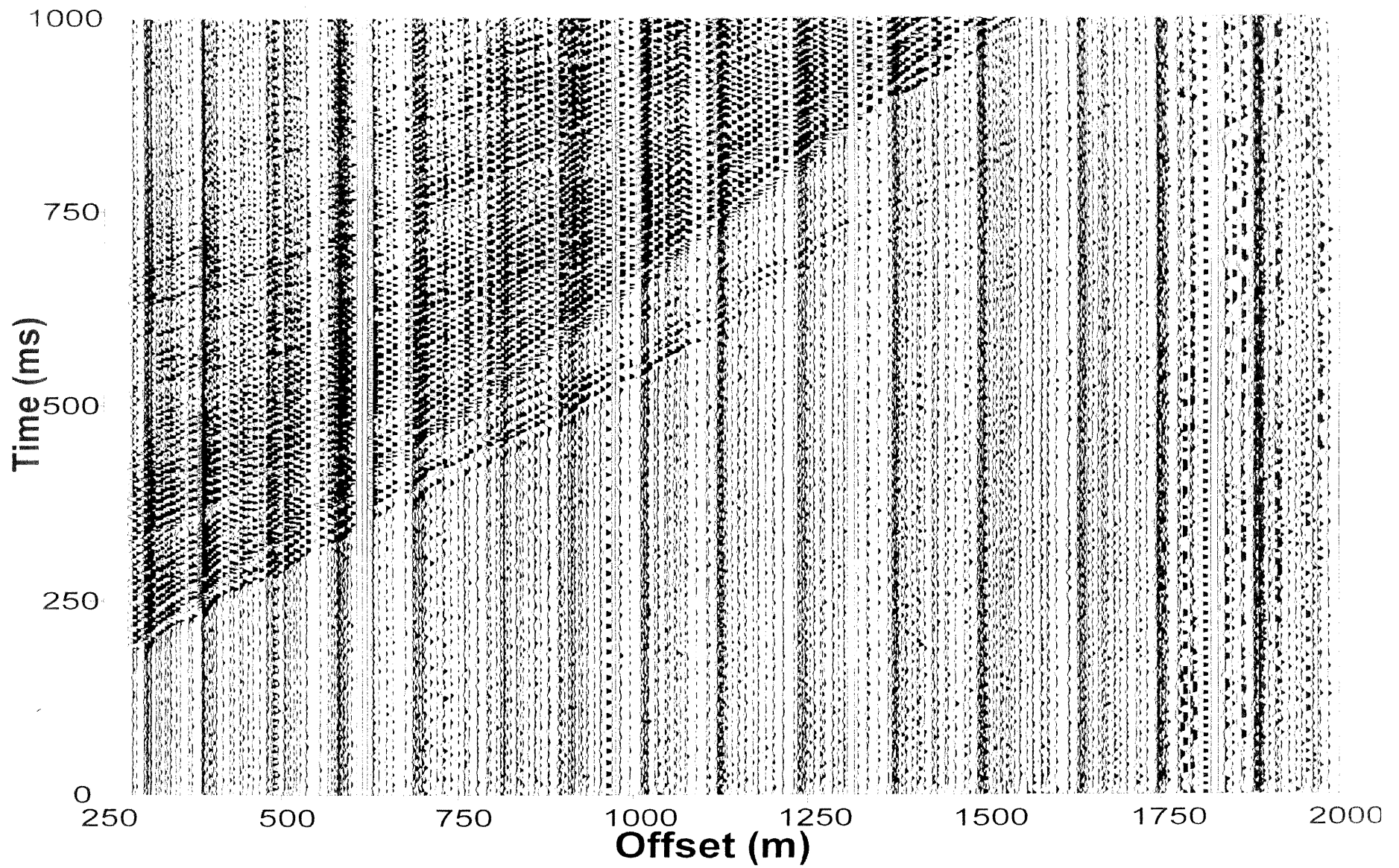


Figure 3.5 Original OBS data recorded from 95-1A, which was deployed in the basin

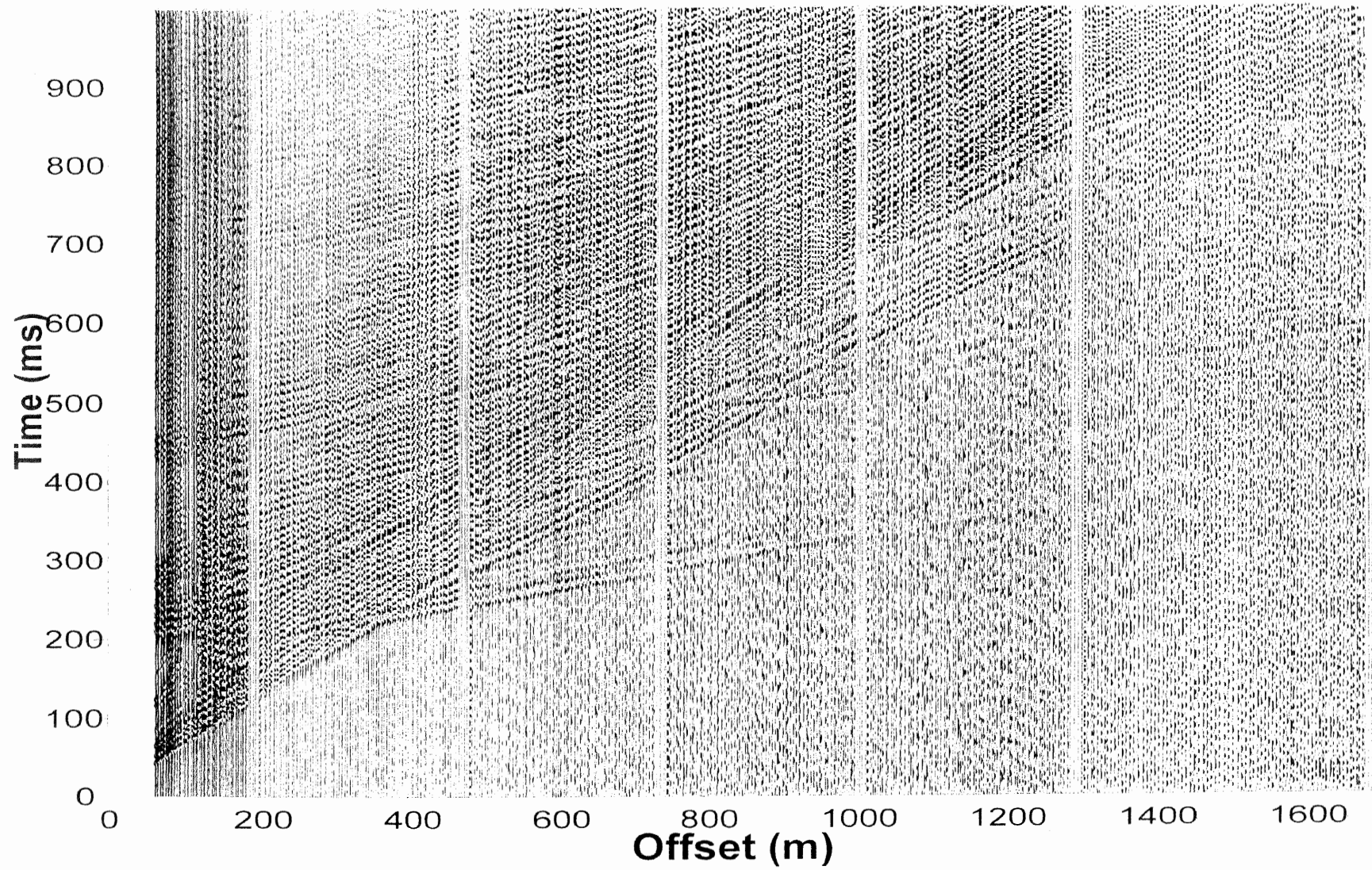


Figure 3.6 Original OBS data recorded from OBS 95-2A, which was deployed on the moraine

Once the velocity structures and the thicknesses at each OBS site were deemed adequate the models were entered as parameters into a subsequent modelling program (SeisWide) (www.phys.ocen.dal.ca/~deping). SeisWide has the capability of creating 2-D models with vertical and horizontal gradients using the raytracing methods of Zelt and Smith (1992). This program also has the capability to overlay the calculated velocity models with the original OBS array. This was done for both sites 95-1A and 95-2A.

3.4 Acquisition Methods of Sleeve-Gun Reflection Data

The sleeve-gun reflection data were collected in 1994 during Bedford Institute of Oceanography cruise HUD94-021 on the *CCGS Hudson* to the central Scotian Shelf. A 40 cu.in. sleeve-gun was used to produce the acoustic signal and a towed hydrophone array was used to retrieve the reflected signal (figure 3.1).

The data are recorded simultaneously on analog magnetic tapes and electro-static recorders, known as an EPC. The EPC was set to a sweep rate of 250ms, with an initial delay of 190 ms to eliminate the travel time recorded through the water. This resulted in a data section that represents a two-way travel time period between 190ms and 440ms. The received signals were filtered between 50 and 500 Hz. A 60 cycle filter is often applied to the data before they are recorded in order to eliminate the noise from the ship's engine and the noise created from the movement of the 25 meter single channel streamer.

In 1994 (HU 94-021) a survey was performed which required the oceanographic ship to travel in an elliptical pattern from the basin to the moraine and back, to achieve the collection of 100 profile lines approximately 20 meters apart. The section of the survey that this project will look at is specific to an area of approximately 30km², in the vicinity of

44°1', 63°1' and 44°6', 63°7' (figure 1.1, 1.2). The position of the ship is determined by differential GPS (Global Positioning System), which is accurate to \pm 4-5 meters.

3.5 Methods of Analysis of Air-Gun Reflection Data

The purpose of analysing reflection profiles was to identify significant horizons and correlate them with known lithological units in order to map the lateral extent of these units in Emerald Basin. The determination of an acoustic velocity model (based on refraction results) was initially required so that the intercept travel-times (from refraction) could be correlated with the reflection profile horizon travel-times.

The first step in analyzing the reflection data required that the survey profiles from cruise HUD 94-021 be displayed with respect to their geographical locations, so that the geographical positions of the reflections could be determined. In order to achieve this a UNIX GIS program, known as *GRASS*, was used (www.baylor.edu/~grass). *GRASS* is a public domain Raster GIS program originally developed by the US Army Corp of Engineers. The same program was used to display the positions of the OBSs, and the survey lines on a bathymetry map of Emerald Basin (figure 1.2). In order to have the navigation positions in a format that would be compatible with the reflection data the navigation data were decimated to one-minute intervals.

The original survey was run at a spacing of 20 meters. To get an overall representation of the study area, and to reduce the size of the data set that would be analyzed, a line approximately every 100 meters (approximately every 5th original line) was chosen in the appropriate vicinity of the OBS recorders (figure 1.2). The lines chosen were 95-15, 95-25, 95-40, 95-50, 95-55, 95-60, 95-65, 95-75, 95-85, and 95-90 (Appendix

1). These lines were chosen on the basis of data availability, data quality and location (approximately every 100 meters).

Six distinguishable horizons were chosen within each reflection profile and the horizons were traced onto mylar paper so that they could be digitized (Appendix 1). The horizons were chosen based on their travel times, which could be correlated with the significant velocity contrasts (previously determined from the refraction data) indicative of lithological changes. The digitizing program assigned each digitized point an x,y coordinate (based on the Julian Day) and a time value (based on travel-time, ranging from 190ms to 440ms).

The digitized files were put into two MATLABTM programs (H. Lau personal communications 2001). The first program changed the Julian Day value assigned during the digitizing process to a UTM coordinate based on the navigation files. The second program was designed to combine the new navigation positions with the two-way travel time (depth) positions for each horizon, within each profile. The resulting files then contained a UTM position, a two-way travel time and a decimated time that represented when the data were recorded. The next program utilized change the UTM coordinates into latitude and longitude coordinates based on a central meridian of -63.

The final program used was GMT (generic mapping tool) (www.soest.hawaii.edu/gmt/gmt/doc/html), with which a 2-dimensional grid was created by correlating the digitized horizons with calculated velocities. This step required the integration of the reflection data with the refraction data. Previously (during synthesis of the velocity model from refraction data) the two-way travel time for each calculated velocity was determined. This information allowed the two-way travel time on the

reflection profile to be correlated with the two-way travel time from the refraction intercept. The unit defined by the horizon on the reflection profile could then be correlated with a velocity (calculated from the refraction data). Based on previous work by Barrett et al. (1964), Bocher (1983), Moran et al. (1989, 1991) and Wade and MacLean (1990), the calculated velocities could be linked with known lithological units, since the horizons on the reflection profile, which correspond to changes in acoustic impedance and therefore also velocity, correspond to changes in lithology. Two tables were created (Tables 4.3 and 4.4, presented in Chapter 4) so that the velocities, travel times and lithological units could easily be correlated. Using the GMT program, contoured thickness maps were created by combining the travel time, position and velocity information gathered for each digitized horizon. The result was a contoured thickness map for each horizon that had a determined top and bottom boundary layer.

CHAPTER 4

RESULTS

4.1 Slope- Intercept Velocity Models

The initial models for this project were based solely on the slopes and intercepts determined from the raw OBS array data (figures 3.5, 3.6). Three velocities were initially recognized from OBS 95-1A. They were 1.49km/s, 1.9km/s and 2.1km/s. Intercepts from these velocities were also determined and with these values the thicknesses of three units were determined. The initial model for OBS 95-1A is summarized in table 4.1. The initial calculations from OBS 95-2A showed velocities of 1.49 km/s, 1.90 km/s, 2.1 km/s and 6.1 km/s, and this velocity model is summarized in table 4.2.

The velocity models were then entered into a modelling program (RayTrace) as parameters, and superimposed onto the digitized points (figures 4.1, 4.2). The purpose of this step was to determine the accuracy of the calculated model. Figure 4.1 was made from OBS 95-1A results, while figure 4.2 was made from OBS 95-2A results. The dotted lines represent the digitized points and the continuous lines represent the calculated velocity model. In figure 4.1 the direct arrival matches well, as do the 1.9 km/s and 2.1km/s values. Likewise in figure 4.2 it is evident that 1.49 km/s is a good match as well as 1.9 km/s, 2.1 km/s and 6.1 km/s. The data and the calculated values correlate well if the continuous lines trace over the digitized points. It is evident that a few arrivals were missed in each case, because there are digitized points that do not have calculated values correlated to them. Due to this fact the models were modified and more complex velocity sequences were generated.

Unit	Velocity	Thickness
1	1.49 km/s	55 m
2	1.90 km/s	37 m
3	2.1 km/s	

Table 4.1- Initial Velocity-Thickness model determined from OBS 95-1A, based on slope-interval results.

Unit	Velocity	Thickness
1	1.49 km/s	39 m
2	1.90 km/s	98 m
3	2.10 km/s	15 m
4	6.10 km/s	

Table 4.2- Initial Velocity-Thickness model determined from OBS 95-2A, based on slope-interval results

EMERALD BASIN OBS 95-1A

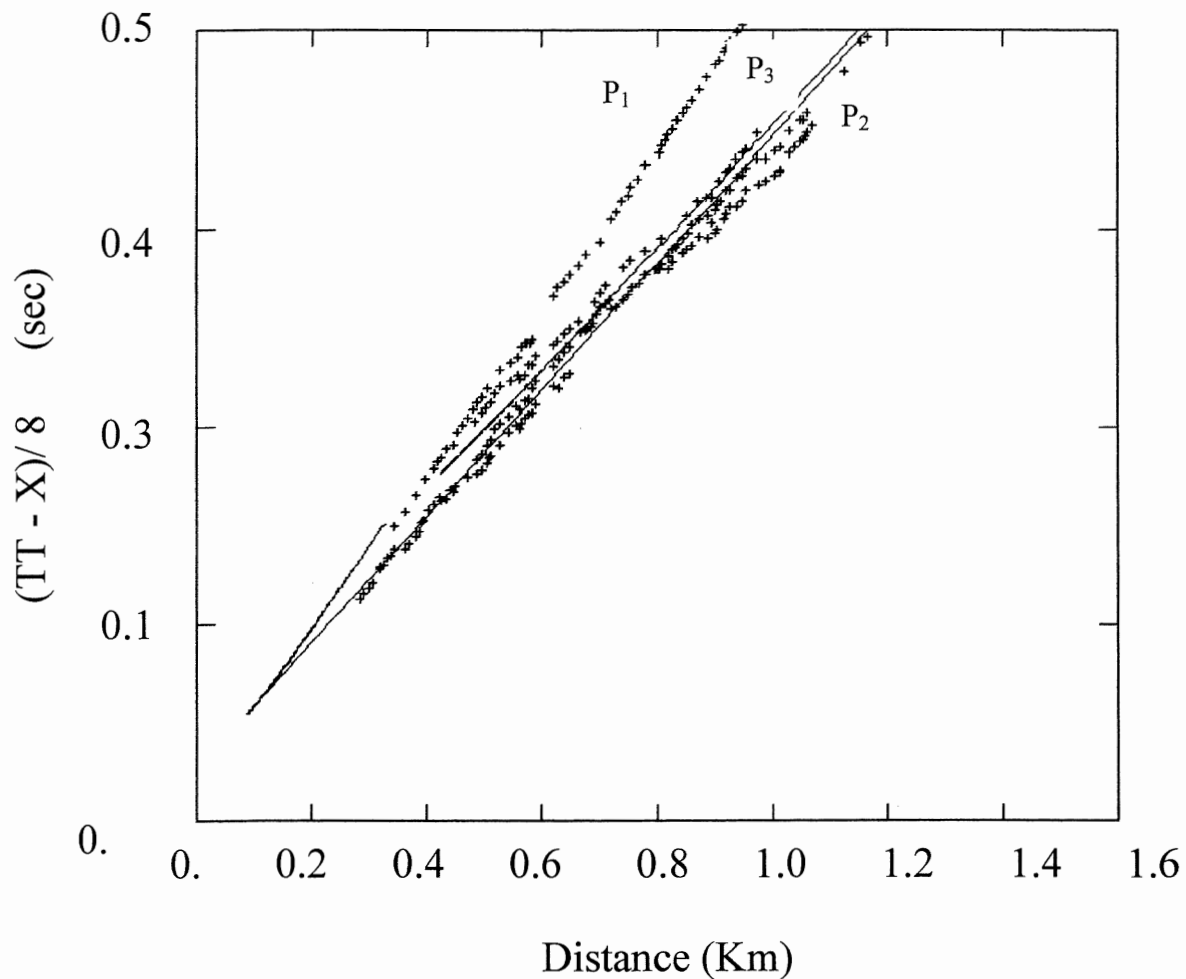


Figure 4.1 Initial velocity model (continuous lines) based on results from the slope intercept calculations, superimposed on the digitized refraction arrays (dots). The x-axis represents distance from the source in kilometers. The y-axis represents the two-way travel times (seconds); the axis has been reduced by a factor of 8 to reduce the slopes, so that the fit can be seen at a larger scale. P₁ represents the direct arrival from the water wave, P₂ represents the second arrival from the 1.9km/s refractor and P₃ represents the refractor with a velocity of 2.1km/s.

EMERALD BASIN OBS 95-2A

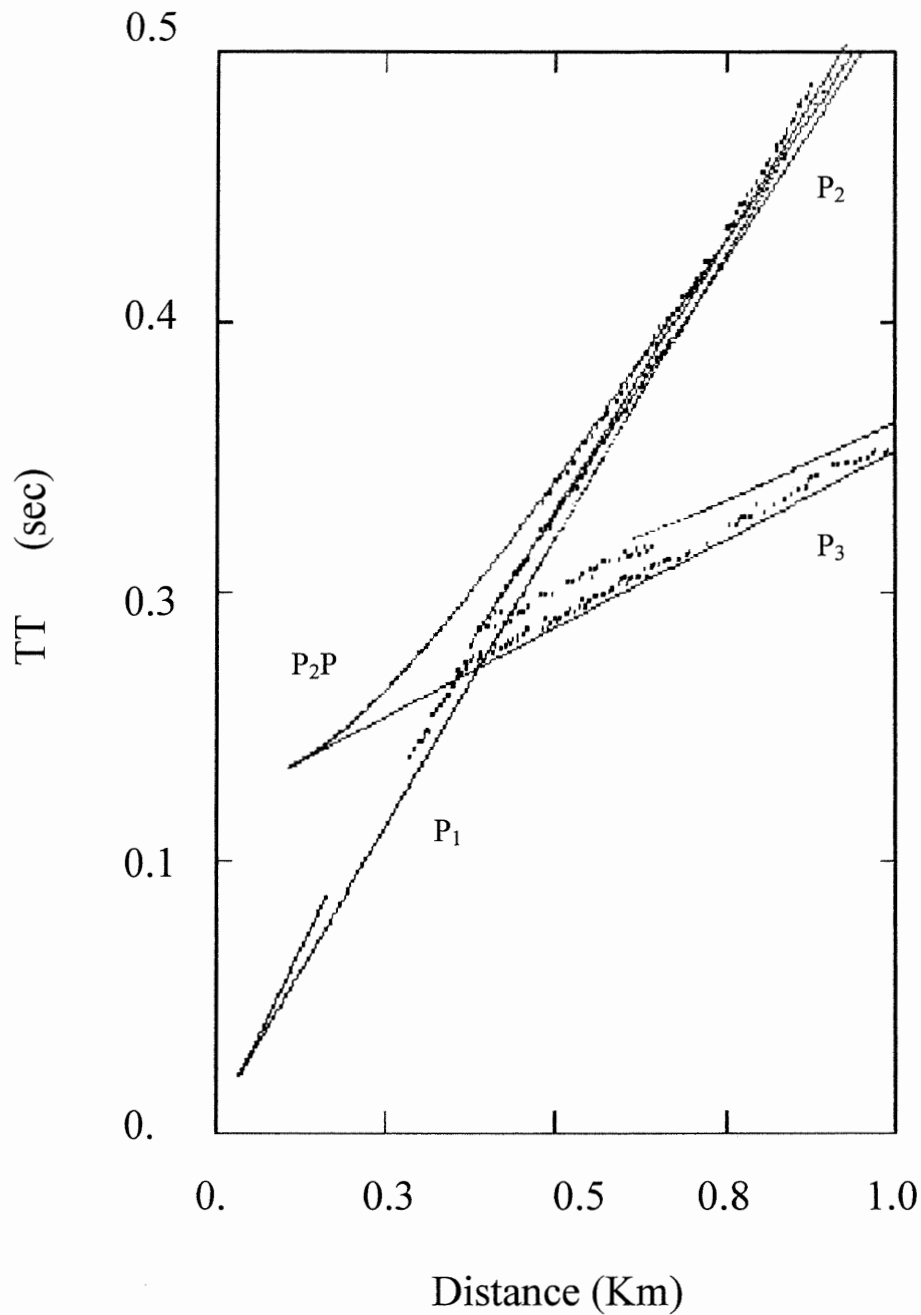


Figure 4.2- Initial velocity model (continuous lines) based on results from the slope intercept calculations, superimposed on the digitized refraction arrays (dots). The x-axis represents distance from the source in kilometers. The y-axis represents the two-way travel times in seconds. P₁ represents the direct arrival from the water wave ($v=1.49$ km/s), P₂ represents the 1.9 km/s refractor, P₃ represents the 6.1 km/s refractor and P₂P represents the initial reflection arrival, which corresponds to the reflection from the seabed interface.

4.2 Velocity – Gradient Models

The significant changes that were made to make the models more accurate was the addition of the Emerald Silt and LaHave Clay layers that were masked, or hidden, due to the fact that their acoustic velocities are lower than that of water. Based on Snell's law the velocity of a layer cannot be determined if it is lower than that of the previous layer. Which is the case in Emerald Basin where the Emerald Silt and LaHave Clay have acoustic velocities lower than 1.49 km/s, which is the acoustic velocity of the water column above. The acoustic velocity information for the LaHave Clay and the Emerald Silt was gathered from previous work, namely that of Moran et al. (1989, 1991).

The new velocity models were used in the SEISWIDE program (www.phys.ocen.dal.ca/~deping), which has the capacity to display 2-D vertical and horizontal gradient models. In order to determine the accuracy of the more complex model, the calculated values were superimposed onto the original data (figures 4.3 and 4.4).

The next step was to correlate the velocity model with the lithological units known to occur in Emerald Basin. In order to form the correlations the author's results were compared with previous velocity measurements recorded on sediments in Emerald Basin by Moran et al. (1989, 1991) and elsewhere on the Scotian Shelf by Barrett et al. (1964) and Brocher (1983). The calculated velocity values generally agreed with the previous identified velocities. The units identified from the reflection profiles and OBS data were therefore easily correlated with the lithological units known to exist in the study area. The correlations are displayed in tables 4.3 and 4.4.

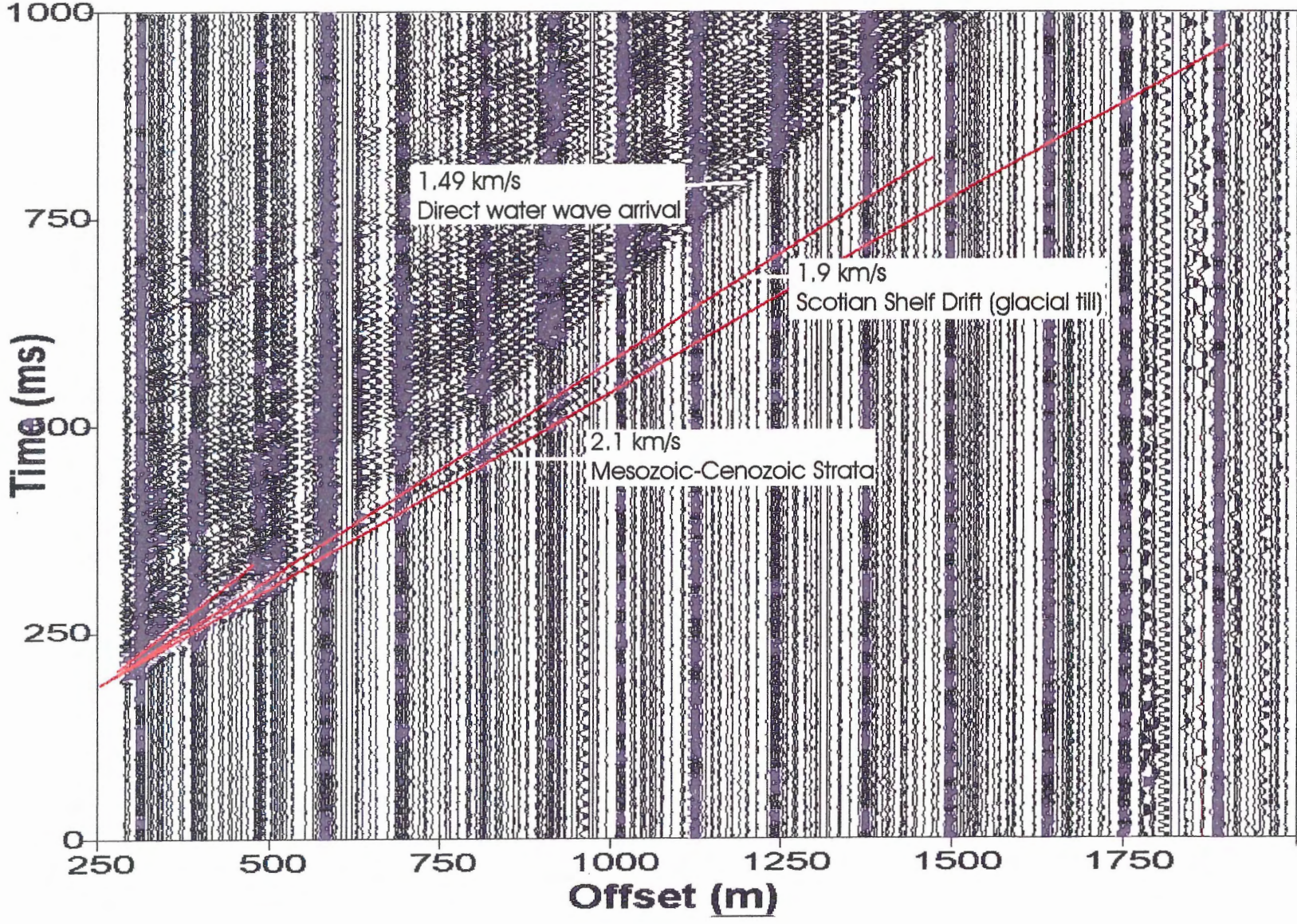


Figure 4.3 Calculated refraction arrivals derived from the proposed velocity model, superimposed on the original OBS 95-1A data.

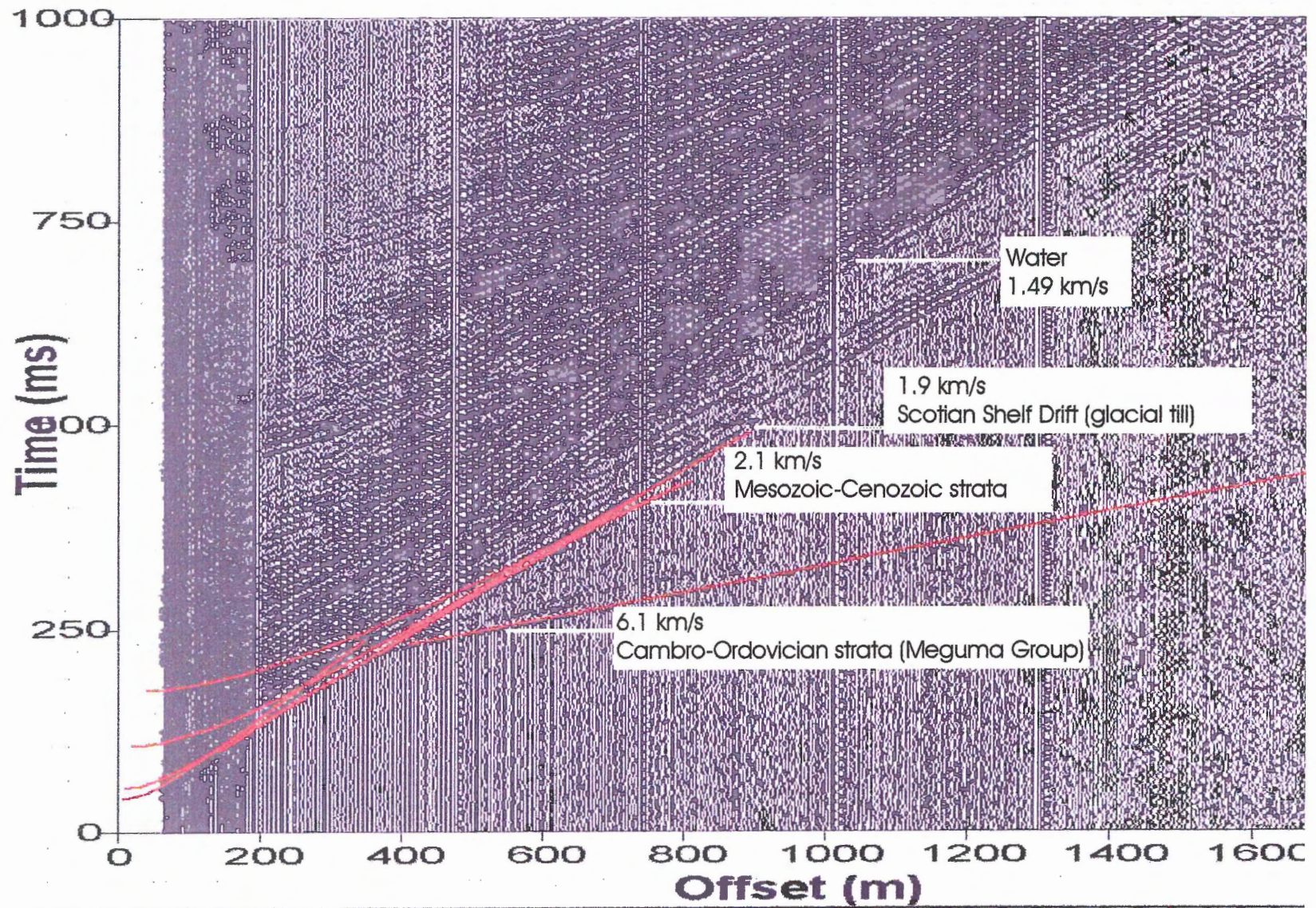


Figure 4.4 Calculated refraction arrivals derived from the proposed velocity model, superimposed on the original OBS 95-2A data.

Horizon	Two-Way Travel Time to the bottom of the horizon (ms)	Velocity (km/s or m/ms)	Lithology	Thickness (m)
Seabed	280-287	1.49	Water	200
H2	286-297	1.44 (based on previous work)	LaHave clay	6
H3	306-313	1.45 (based on previous work)	Emerald silt	12
H4	329-338	1.90	Scotian Shelf Drift	16-22
H5	464 (based on previous work)	2.1	Mesozoic-Cenozoic strata	143
H6		6.1	Meguma Group basement	

Table 4.3 Summary table of the velocities and thicknesses of the lithological units associated with OBS 95-1A, in the basin.

Horizon	Two-Way Travel Time to the bottom of the horizon (ms)	Velocity (km/s or m/ms)	Lithology	Thickness (m)
Seabed	206-230	1.49	Water	175
H2		1.44	LaHave clay	0
H3		1.45	Emerald silt	0
H4	257-276	1.90	Scotian Shelf Drift	42-60
H5	342-351	2.1	Mesozoic-Cenozoic strata	84
H6		6.1	Meguma Group basement	

Table 4.4 Summary table of the velocities and thicknesses of the lithological units associated with OBS 95-2A, on the moraine.

4.3 Sediment Thickness Models

Once the author was confident with the velocity model the GMT (www.soest.hawaii.edu/gmt/gmt/doc/html) program was utilized to display the results as sediment thickness models representative of each horizon chosen from the reflection data. Figure 4.5 represents the contoured depth to the seabed. The values show that the depth varies from 170 meters on the moraine to a depth of 210 meters in the basin.

Figure 4.6a displays the thickness calculated for the unit with a velocity of 1.44 km/s, which represents the LaHave Clay. This thickness model shows that the unit is only present in the basin, since there is a value of zero in the north-western corner where the moraine exists. The LaHave Clay has a uniform thickness of about 6 meters within the basin study area.

Figure 4.6b represents the thickness of the Emerald Silt unit, with a velocity of 1.46 km/s. The thickness for this unit range from 0-12 meters, and similarly to the LaHave Clay it is present exclusively in the basin. The distinction between Emerald Silt facies A and facies B cannot be made because the difference in acoustic velocities is insignificant and the resolution of the reflection profile is not high enough to distinguish between the facies. The facies are characterized based on depositional time and style and not on acoustic velocity.

Figure 4.6c represents the thickness of the Scotian Shelf Drift, a glacial till. This unit is present across the entire study area, and its thickness ranges from 16 meters (in the basin) to 50 meters (within the moraine). This was the final mappable layer within the study area, due to the depth that the reflection data were able to penetrate. The next horizon determined on the reflection profiles represents the top of the bedrock but the

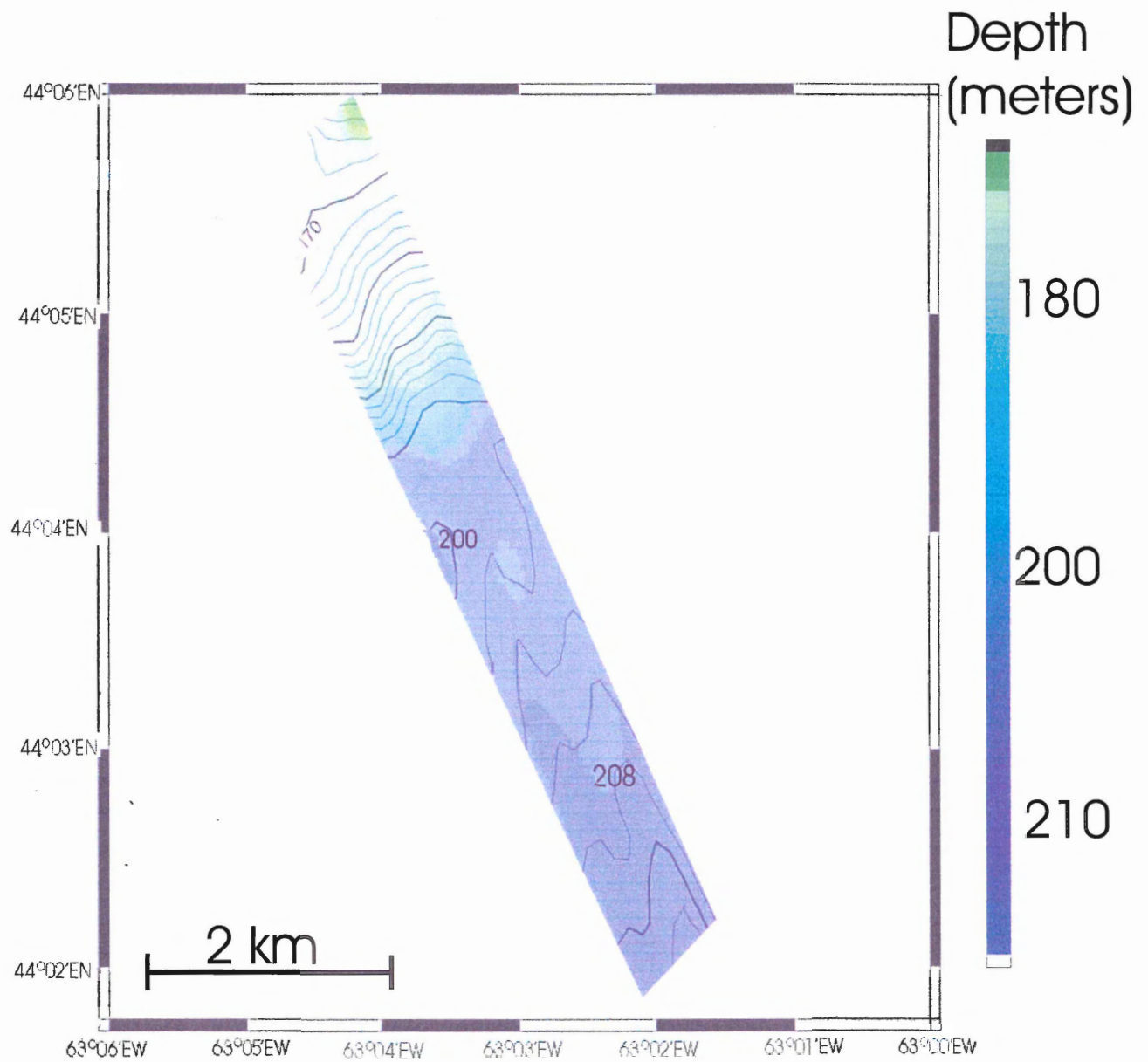


Figure 4.5 A contoured depth plot of the seabed. Depths range from 170 meters on the moraine down to 210 meters in the basin.

Figure 4.6a Contoured thickness map of the LaHave Clay unit in Emerald Basin

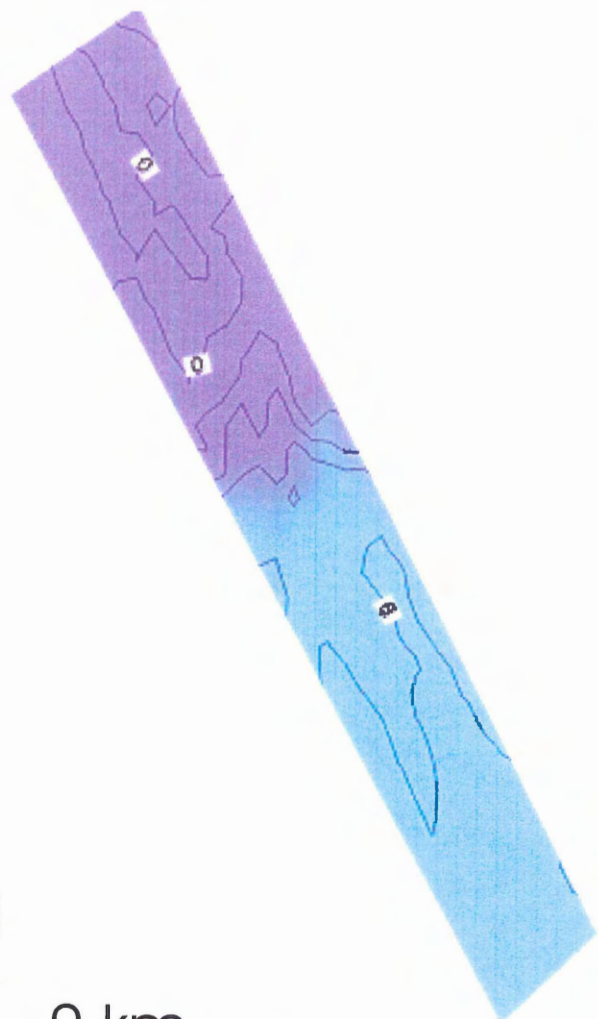
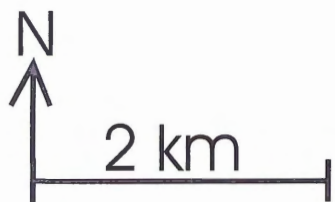
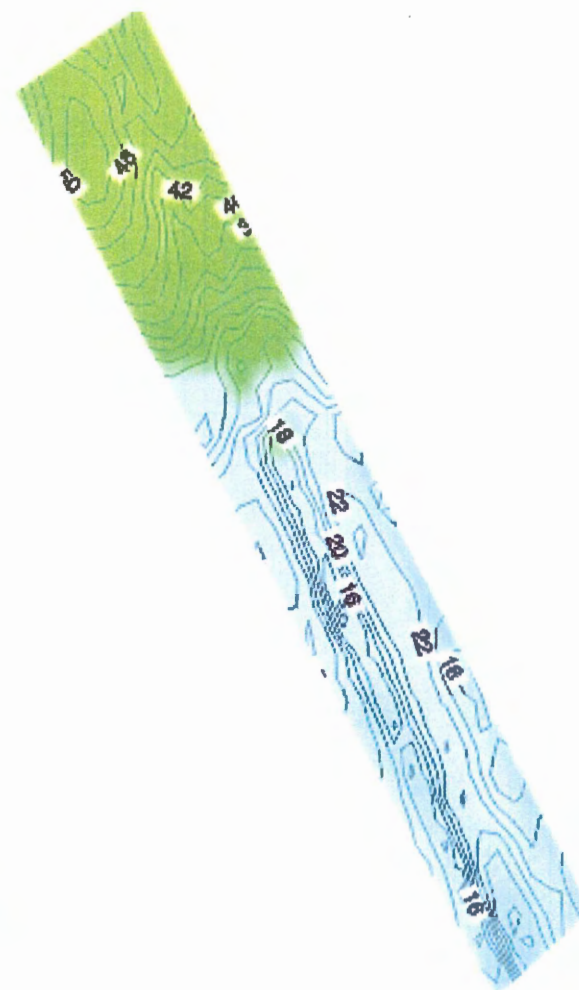


Figure 4.6b Contoured thickness map of the Emerald Silt unit in Emerald Basin



Figure 4.6c Contoured thickness map of the Scotian Shelf Drift, glacial till unit, in Emerald Basin



lateral extent of the boundary could not be mapped because it is not defined within the basin.

4.4 Sources of Error

The margins of error for the acoustic velocities were determined by conducting least-squares statistical regression analysis on the digitized points that were used in the slope-velocity calculations. Errors within the velocities would effect the accuracy of the determined thicknesses, since the thicknesses were calculated based on the equation:

$$D = v \cdot t \quad \text{where } D = \text{thickness,} \\ \quad \quad \quad v = \text{velocity,} \\ \quad \quad \quad t = \text{travel time}$$

The margin of error statistically determined for the Scotian Shelf Drift unit, which has a calculated velocity of 1.9 km/s, is ± 0.01 km/s, for both the basin (95-1A) and the moraine (95-2A) data. This margin of error is based on a slope uncertainty of 0.0027s/km (on the basin data) and 0.0023 s/km (on the moraine data) and an intercept uncertainty of 0.0018 sec (on the basin data) and 0.0014 sec (on the moraine data). The Mesozoic-Cenozoic strata, which have a calculated velocity of 2.1 km/s, contain a margin of error of ± 0.03 km/s from the basin data and a margin of error of ± 0.01 km/s from the moraine data. The basin analysis is based on a slope uncertainty of 0.0075 s/km and an intercept uncertainty of 0.0067 sec. The moraine analysis is based on a slope uncertainty of 0.0017s/km and an intercept uncertainty of 0.0018 sec. The 6.1 km/s velocity, from the Cambro-Ordovician strata (Meguma Group basement), which was only detected on 95-2A (moraine position) data has a statistically calculated error of ± 0.03 km/s. This margin

of error is based on a slope uncertainty of 0.0008 s/km and an intercept uncertainty of 0.0005 sec.

Errors in the thicknesses of the lithological units could also arise if the horizons were not chosen or digitized accurately, or if the travel times were not correlated correctly with the calculated velocities. These errors would result in inaccuracies within the shapes of the contours as well as the position and depth of the boundaries.

The author assumed that the parallel reflections present on the sleeve-gun reflection profiles were multiples (figure 4.7), especially in the case of the Emerald Silt boundary. However, if the preceding assumption is false, and the parallel reflectors represent different phases or laminations within the unit, then the Emerald Silt unit is actually thicker than the 0-12 meters suggested by the author.

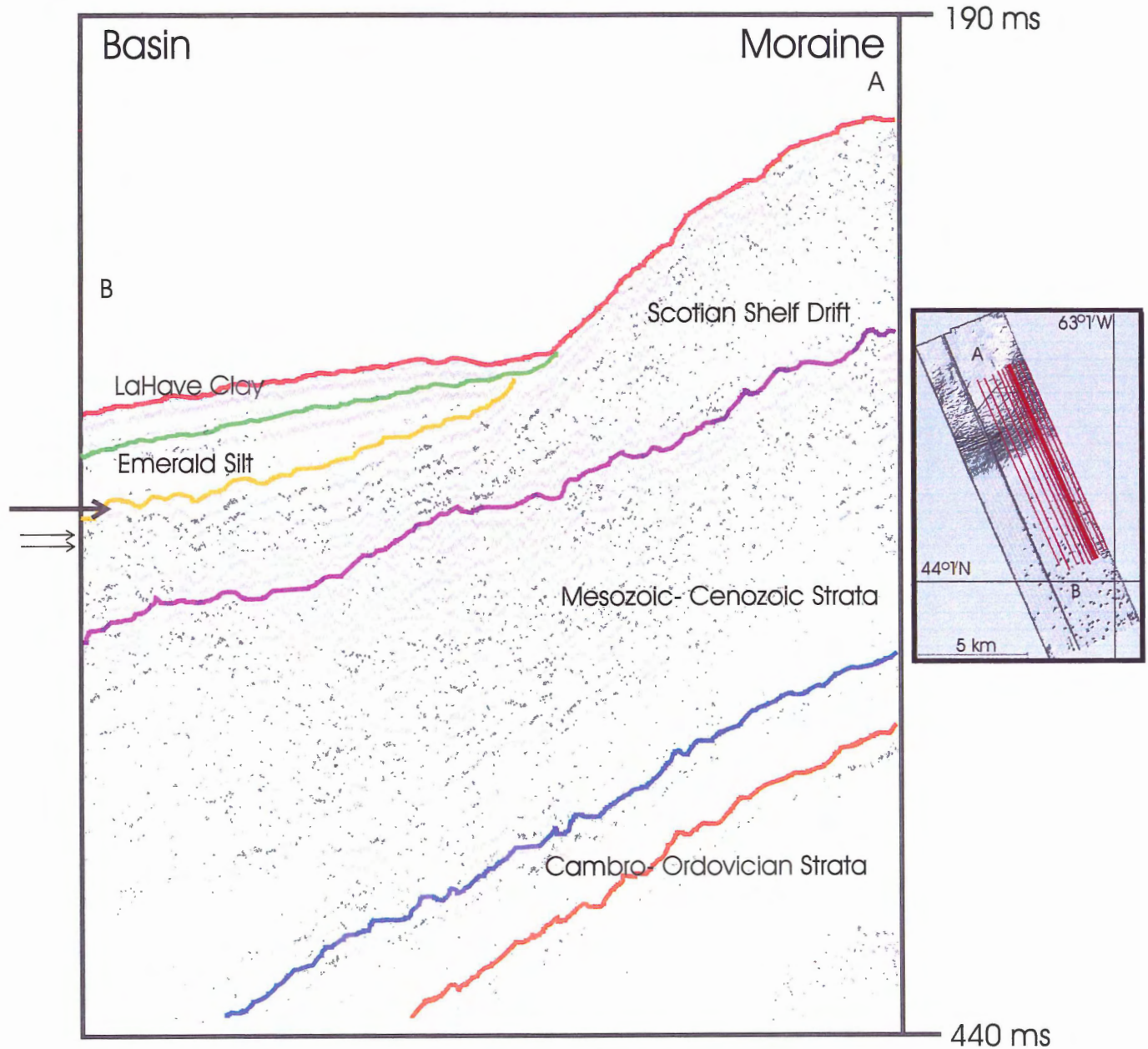


Figure 4.7 Example profile from the basin to the moraine (exact location shown on small map to the right) illustrating the horizons chosen and the horizons interpreted as multiples. The large arrow indicates the horizon chosen as the Emerald Silt boundary, while the small arrows indicate the horizons interpreted as multiples.

CHAPTER 5

INTERPRETATIONS and CONCLUSIONS

5.1 Velocity Models

The initial calculations using the slope intercept method yielded velocities of 1.49 km/s, 1.9 km/s and 2.1 km/s for OBS 95-1A. Four velocities were determined for OBS 95-2A: 1.49 km/s, 1.9 km/s, 2.1 km/s and 6.1 km/s. The direct arrival from each OBS yielded a velocity of 1.49 km/s, which is known to represent the seawater since this value was initially used to calibrate the offset of the instrument. The values of 1.9 km/s and 2.1 km/s were evident on both OBS sites, therefore it was determined that they must represent lithological units that are present both in the basin and in the moraine position. The OBS 95-2A array displayed an arrival which had a unique high velocity of 6.1 km/s. High velocities are representative of dense, consolidated strata, while strata that are less consolidated and less compacted will have a lower velocity signature. Therefore, it was inferred that the 6.1 km/s must represent a deeper bedrock unit.

Based on previous work completed in Emerald Basin (Brocher 1983; Wade and MacLean 1990) high velocities of 5.5 km/s to 6.15 km/s were reported to represent the Cambro-Ordovician Meguma Group strata; therefore it is the opinion of the author that the calculated velocity of 6.1 km/s correlates with the Cambro-Ordovician Meguma Group strata. Previous work done by Moran et al. (1989, 1991) determined physical properties for the upper sedimentary layers in Emerald Basin from core samples. These previous studies determined that the LaHave Clay has an acoustic velocity of 1.44 km/s and the Emerald Silt has an acoustic velocity ranging from 1.45 km/s to 1.46 km/s. The velocity can vary slightly depending on the location of the sediment. For example, the

Emerald Silt of core 87-003-002 (figure 1.1 and 5.1) has an average velocity of 1.45 km/s, whereas the silt from core 87-003-004 (located at a greater depth) has a velocity of 1.46 km/s. The LaHave Clay and the Emerald Silt have velocities lower than that of water because they are extremely unconsolidated and have a high water content. The refracted arrivals for these low velocity sediments are not present on the OBS arrays because they were “masked” by higher velocity of the water arrival. As previously mentioned (in chapter 4) due to the mathematical properties of Snell’s law, the refractions from a layer with a lower velocity than that of the previous layer will not be recorded. Since the velocities for the LaHave Clay and the Emerald Silt were undeterminable from the OBS data due to this fact, the values stated by Moran et al. (1991) were used for modeling procedures.

Huntec seismic profiles were also used to gain more detailed information about the upper lithological units present in Emerald Basin since the resolution of these profiles is much greater (figures 5.1). These profiles provided the opportunity for visual correlations to be made between the thicknesses of the units and the travel times.

Based on seismic studies performed by Brocher (1983) and Moran et al. (1991) the calculated acoustic velocity of 1.9 km/s was correlated with the Scotian Shelf Drift, glacial till, deposit. The 2.1 km/s velocity was correlated with the Mesozoic-Cenozoic strata based on Brocher (1983) who reported measured velocities of 2.0- 3.4 km/s for such sediments on the Scotian Shelf.

Summaries of the lithologies and their thicknesses present at each OBS site are outlined in tables 4.3 and 4.4. Comparing tables 4.3 and 4.4 it becomes evident that the same lithological units are not present at each site. OBS 95-1A, which corresponds to an

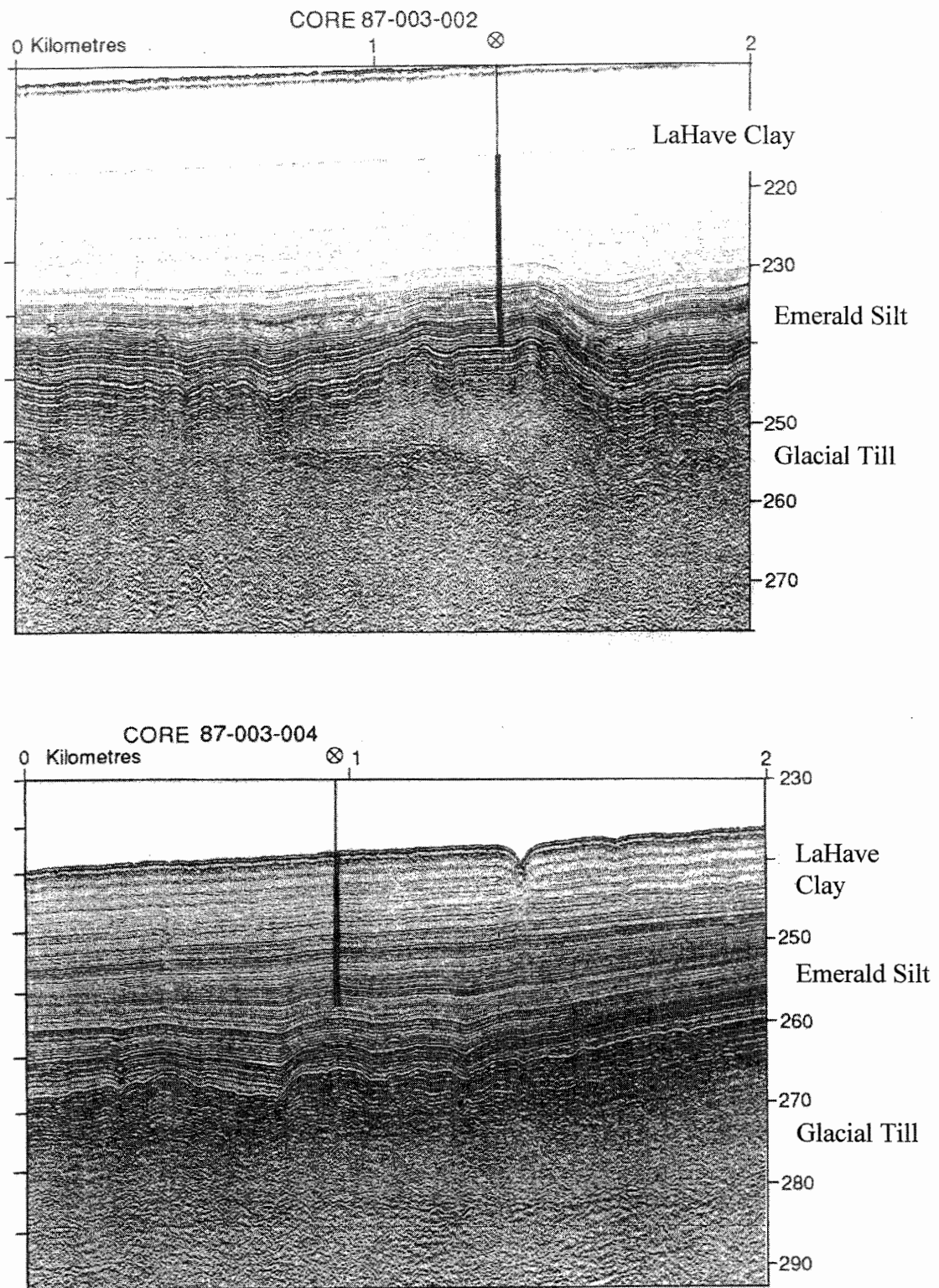


Figure 5.1 Hunttec Profiles from the 1987 core sites 87-003-002 and 87-003-004. The Hunttec reflection data has a higher resolution than the air-gun reflection data which makes the recognition of the shallow Emerald Basin sediments, such as the LaHave clay and the Emerald silt much clearer.

area in the basin has velocities of much lower ranges and contains the lithological units of LaHave Clay, Emerald Silt, the Scotian Shelf Drift and the Mesozoic-Cenozoic sedimentary strata. Conversely OBS 95-2A does not contain the lithological units of LaHave Clay or Emerald Silt but it does contain the Scotian Shelf Drift, the Mesozoic-Cenozoic strata as well as a high velocity unit, representative of the Cambro-Ordovician Meguma Group strata.

The high velocity refractor was not evident on OBS 95-1A, from within Emerald Basin, however, based on previous work completed by Louden (1994) it can be concluded that this lithological unit is present in the basin but at such a depth that it was undeterminable on the OBS array. It was also not evident on the reflection profiles analyzed for this project because they were set to record reflections for 250 ms between 190 ms and 440ms, which meant that any reflectors occurring below 440 ms were not seen.

During CFAV QUEST Cruise 211 in 1994 Ocean Bottom Seismometer data and reflection profiles were collected in Emerald Basin (figure 5.2). This study used a 40 cu. inch air-gun and was able to record a deep reflection at a depth of 464 ms (in two-way travel time) (figure 5.2). The reflection line was run from approximately 44° 1' North 63°5' West to 44° 1' North 62° 5' West. The refraction data was analyzed and the velocity correlating to the deep reflector was determined to be 5.5 km/s (Louden 1994). This value is representative of the Meguma Group strata (based on MacLean and Wade 1990). This information leads to the suggestion that the Meguma Group strata do continue in the basin. Further evidence that the previously mentioned reflector from the QUEST Cruise 211 correlates with the reflector that the author determined represents the

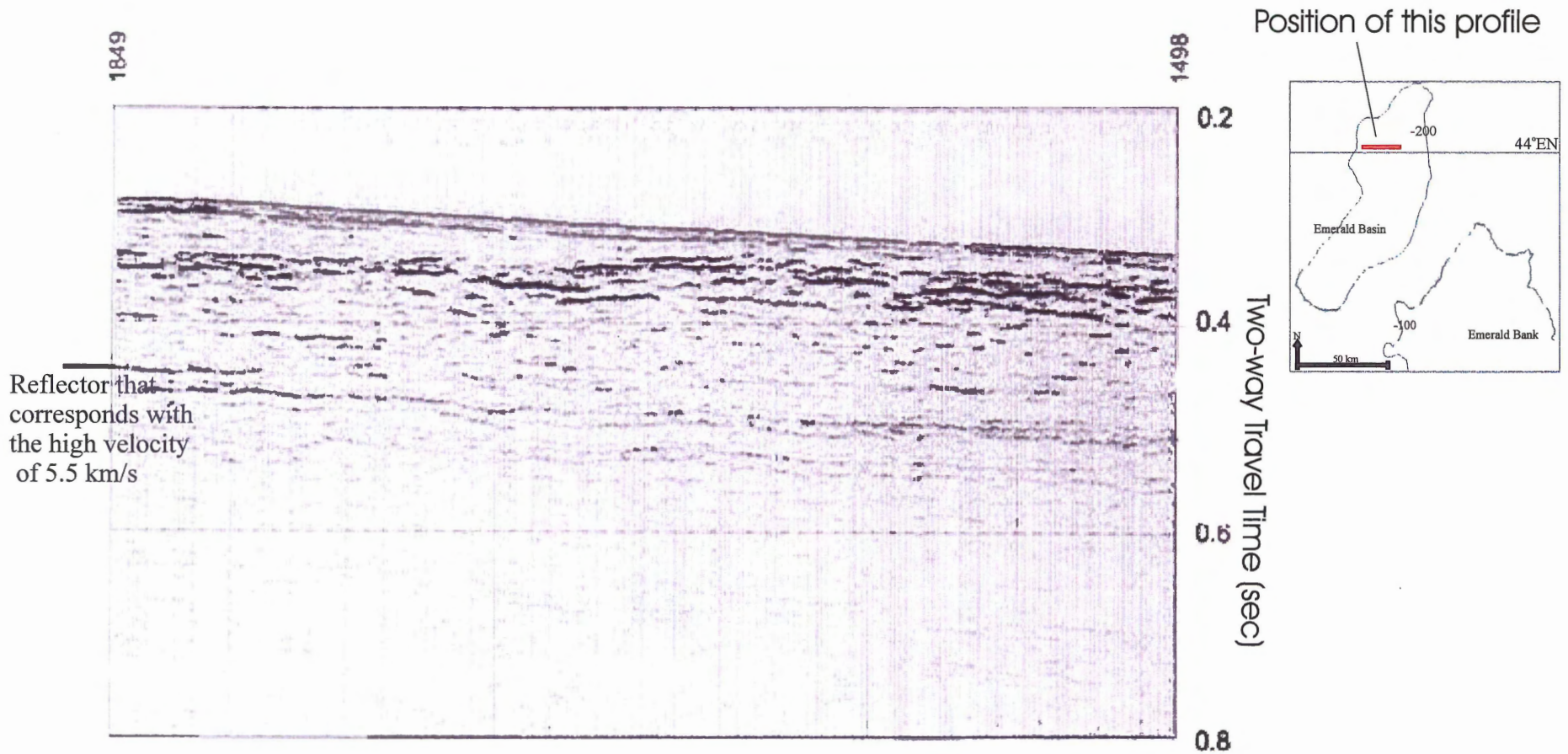


Figure 5.2 Deep seismic profile recorded in 1994 during CFAV QUEST cruise 211. This profile shows evidence that the high velocity refractor, correlated with the Meguma Group basement strata, is present within Emerald Basin. The reflection which has a two-way travel time of 464 ms was determined to represent the Meguma Group basement. Note that the reflector occurs as a couplet.

Meguma Group bedrock, is the fact that the reflectors appear in couplets on both reflection profiles.

The fact that the Meguma Group horizon is present at a greater depth in the basin suggests that the basement strata are dipping to the southeast (down into the basin) and that the Mesozoic-Cenozoic strata are located above. The dipping behaviour of the Meguma Group could be a result of faulting. There are many normal faults on the Scotian Shelf, which are a result of the rifting that occurred during the Mesozoic (Keen et al. 1990).

The results of this project agree with the previous lithological model proposed by King and Fader (1986) (figure 2.1), where the Scotian till is present across the entire area and the LaHave Clay and Emerald Silt are confined to the basins. Figure 2.1 also illustrates the boundary of the Mesozoic-Cenozoic strata and the steeply dipping behaviour of the Meguma Group from under the moraine.

5.2 Thickness Variation Models

The contoured thickness sections created demonstrate that the lithological layers get thicker deeper in the section. Figures 4.6a and 4.6b which represent the LaHave Clay and the Emerald Silt units respectively confirm that these units are only located in the basin and not over the moraine. The LaHave Clay unit is uniform across the basin area and diminishes to a value of zero towards the edge of the moraine. The simple structure of this unit indicates that the depositional environment was quiet, without many depositional influences from storms or currents. The Emerald Silt unit is also quite uniform ranging from 8 to 12 meters within the basin. Due to the limited resolution of the

data analyzed, the distinction between Emerald Silt facies A and facies B cannot be realized. Which also means that evidence to suggest the presence of till-tongues cannot be realized.

Figure 4.6c represents the Scotian Shelf Drift unit. Within this unit the thickness varies from 16 meters in the basin to 48 meters in the northern section where the moraine exists. This relates to the fact the Scotian Shelf Drift is the primary component of the end-moraine complex. The large value of 48 meters represents the thickness of the moraine.

The thickness of the Mesozoic-Cenozoic strata, which was correlated with the calculated velocity of 2.10 km/s, could not be modelled because the lower boundary, which corresponds to the top of the Meguma Group, could not be defined across the entire reflection profile. However, a thickness below the moraine can be calculated based on the average travel times to the Meguma Group reflector. The average twtt of 346 ms was divided by two (173 ms) and then the average one-way travel time from the layer above (133 ms) was subtracted from it, in order to find a value indicative of the one-way travel time through the layer. This value of 40 ms was then multiplied by the velocity of the Mesozoic-Cenozoic strata (2.1 km/s) to acquire a thickness for the unit. This calculation results in an average thickness of 84 meters for the Mesozoic-Cenozoic strata below the moraine. By adding the thickness of the preceding unit, the average depth to the Meguma Group basement, under the moraine, is 135 meters.

According to the reflection profile acquired during CFAV QUEST Cruise 211 in 1994 the high velocity reflection occurs at a two-way travel time of 464 ms (figure 5.2). This value can be used in accordance with the travel time value for the upper boundary of

the Mesozoic-Cenozoic strata to give a total thickness in the basin of 143 meters. Adding this thickness to the thicknesses of the preceding layers, the average depth to the Meguma Group basement, in the basin, is 180 meters.

5.3 A Comparison of Thickness Models

Osler and Chapman (1996) determined a thickness model for the upper sedimentary units in Emerald Basin based on the acoustic shear-wave (s-wave) velocities for the LaHave Clay and the Emerald Silt. The acoustic parameters that they set for the compressional-wave (p-wave) speed were 1.49 km/s for the water, 1.45 km/s for the LaHave Clay, 1.55 km/s for the Emerald Silt and 1.8 km/s for the glacial till (Scotian Shelf Drift). The thickness model that Osler and Chapman (1996) propose states that the LaHave Clay is 9 meters thick and that the Emerald Silt is 29 meters thick. The model proposed by the author is similar with respect to the LaHave Clay value, however, the value that Osler and Chapman proposed for the Emerald Silt is approximately 2.5 times greater than the author's value of 12 meters. This discrepancy could arise from the differences in position in which the two studies were completed. The Emerald Silt unit is known to be thicker in central Emerald Basin, which is where the experiment completed by Osler and Chapman (1996) was performed.

5.4 Implications of Results

A theory on basin and moraine formation could be drawn from the thesis results and interpretations. The Meguma Group strata are the “hardest” of the lithological units found in the Emerald Basin area. At the time of Wisconsinan glaciation the Meguma Group strata would have been located at a higher elevation under the current moraine position (based on the current depth to bedrock of 135 meters) than in the basin (where it is found at 180 meters depth). During Wisconsinan deglaciation the ice remained anchored on topographic highs for extended periods of time (Gipp 1993). The boundary between the Meguma Group and the Mesozoic-Cenozoic would have provided an environment of topographic contrast, with the Meguma Group providing the topographic high for ice to be anchored. During ice sheet retreat large amounts of sediments were deposited during melt-out. If the ice sheet was grounded on the higher Meguma Group zone this would determine the reason for sub-glacial and pro-glacial sediments, such as the Emerald Silt facies A and B, to be located exclusively within the basin. The grounded behaviour of the ice sheet would also have caused an excess of till to be deposited under the point of anchorage. This would explain the position of the moraine, which is comprised dominantly of glacial till.

Controversy could arise from this interpretation because it is unclear whether the Meguma Group was a topographic high at the time of Wisconsinan deglaciation. Other possibilities on basin formation stem purely from the distribution of the glacial till and would not require the influence of pre-existing structures in the bedrock. In this situation the depression of the basin would have been created primarily by the fact that the glacial till coverage in that area was thinner in the vicinity of the basin, creating a low into which

the Emerald Silts could be deposited. However, based on the tectonic history of the Meguma Group and the fault complex that exists throughout the boundary area, it is the opinion of the author that the Meguma Group was positioned as a topographic high during the Wisconsin glacialiation and therefore was the dominant factor that affected the distribution of the glacial sediments.

5.5 Conclusions

The lithological units in Emerald Basin were characterized acoustically based on Ocean Bottom Seismometer refraction data and sleeve-gun reflection profiles. The thicknesses of the LaHave Clay, Emerald Silt, Scotian Shelf Drift and the Mesozoic–Cenozoic units were calculated, and the thicknesses of the LaHave Clay, Emerald Silt and Scotian Shelf Drift were contoured and mapped. In comparison with other thickness models derived from s-wave OBS data, the author's thickness model for the upper sedimentary unit, namely the LaHave Clay and the Emerald Silt is comparable. Unfortunately the thickness of the Mesozoic-Cenozoic strata could not be mapped because the underlying boundary, the Meguma Group bedrock, could not be determined across the entire project area. However, the depth down to the Meguma Group bedrock was determined, with the aid of previous studies and it was found to be 135 meters under the moraine and 180 meters in the basin. The difference in these depth values led the author to conclude that the tectonic history affected the shape of the bedrock, which in turn affected the deposition of the subsequent sedimentary deposits.

The following summary can be made for the formation of Emerald Basin based on the determined thicknesses, depths and positions of the lithological units.

- Tectonic history, namely rifting and faulting, on the Scotian Margin created a topographic high within the Meguma Group under the current position of the moraine (evident in the depth contrast to bedrock between the moraine position, 135 meters, and the basin position, 180 meters).
- During Wisconsinan deglaciation the ice sheet retreated and was temporarily anchored on topographic highs, such as the Meguma Group strata.
- Glacial washout occurred while the ice sheet was temporarily anchored and caused the depression of the basin to become “overdeepened” from the carving effects of the melt-waters.
- A thick deposit of glacial till developed while the ice was anchored, and created the end- moraine complex located on the high side of the Meguma boundary at the northern edge of the basin.
- Sub-glacial Emerald Silt facies A was deposited during recession and the pro-glacial Emerald Silt facies B was deposited into the “overdeepened” depression while the ice was anchored to the northeast, explaining the exclusive position of these units within the basin area.
- Finally, during the relative sea level rise that accompanied the post-glacial time period, the LaHave Clay was deposited in a ponded style, into the basin from the winnowing glacial material left on the banks and adjacent land areas.

5.6 Recommendation for Further Work

The depth and boundary of the Meguma bedrock could be mapped if the seismic data penetrated to a greater depth. Having access to digital data files would make manipulation of the seismic data easier, and could allow the thickness variations to be mapped as 2-D cross sections. Dealing with the data in two dimensions would provide greater details about the horizontal and vertical variations within the lithological units. Investigations and comparisons of the data collected from the other four OBSs (B-E) could also provide a more detailed map of the horizontal changes in the velocity structures.

REFERENCES

- Amos, C.L., and Miller, A.A.L. 1990. The Quaternary stratigraphy of the southwest Sable Island Bank, eastern Canada. *Geological Society of American Bulletin*, **102**: 915-934.
- Barrett, D., Berry, M., Blanchard, J., Keen, M., McAllister, R. 1964. Seismic studies on the eastern seaboard of Canada: the Atlantic coast of Nova Scotia. *Canadian Journal of Earth Sciences*, **1**: 10-22.
- Brocher, T.M. 1983. Shallow crustal structure of the continental margin off Nova Scotia. *Canadian Journal of Earth Sciences*, **20** (11): 1657- 1672.
- Benn, D., and Evans, D. 1998. *Glaciers and Glaciation*. London, New York: New York: Arnold and Wiley, 734p.
- Fader, G.B.1991. Surficial geology and physical properties 5: surface features. *In East Coast Basin Atlas Series: Scotian Shelf*; Atlantic Geoscience Center, Geological Survey of Canada, p.117.
- Gipp, M., and Piper, D. 1989. Chronology of Late Wisconsinan glaciation, Emerald Basin, Scotian Shelf. *Canadian Journal of Earth Sciences*, **26**: 333-335.
- Gipp, M.R. 1993. The orientation of buried iceberg scours and other phenomena. *Marine Geology*, **114**: 226-272.
- Gipp, M.R. 1993 b. "Lift-off" moraines: evidence for ice rises and interlobate moraines on the Scotian Shelf, Canada. *Geological Society of America- Abstracts with Programs*, **25** (6): 158.
- Gipp, M.R. 1994. Late Wisconsinan deglaciation of Emerald Basin, Scotian Shelf. *Canadian Journal of Earth Sciences*, **31**: 554-566.
- Gipp, M. R. 1998. Late Wisconsinan buried iceberg scours in Emerald Basin, Scotian Shelf. *Geological Society of America- Abstracts with Programs*, **20** (1): 22.
- Hall, F., Miller, A., Moran, K. 1998. Deglaciation of the central Scotian Shelf: foraminifera, physical properties and acoustic records from Emerald Basin. *Geological Society of America- Abstracts with Programs*, **30** (1): 23.
- Jansa, L.F. and Wade, J.A. 1975. Paleogeography and sedimentation in the Mesozoic and Cenozoic, Southeastern Canada. *Canadian Society of Petroleum Geologists Memoir*, **4**: 79-102.

- Josenhans, H.W., King, L.H., and Fader, G.B. 1978. A sidescan sonar mosaic of pockmarks on the Scotian Shelf. *Canadian Journal of Earth Sciences*, **15**: 831-840.
- Keen, C.E., Loncarevic, B.D., Reid, I., Woodside, J., Haworth, R.T., Williams, H. 1990. Tectonic and geophysical overview. *In* *Geology of the Continental Margin of Eastern Canada*, Geological Survey of Canada; **2**: 31-85.
- King, L.H. and MacLean, B. 1970. Pockmarks on the Scotian Shelf. *Geological Society of America Bulletin*, **81**: 3141-3148.
- King, L. H., and Fader, G. B. J. 1986. Wisconsinan glaciation of the Atlantic continental shelf of southeast Canada. *Geological Survey of Canada, Bulletin* 363.
- King, L. H. 1993. Till in the marine environment. *Journal of Quaternary Science*, **8** (4) 347-358.
- King, L. H. 1996. Late Wisconsinan ice retreat from the Scotian Shelf. *Geological Society of America Bulletin*, **108** (8): 1056-1067.
- King, E, L. 2001. A glacial origin for Sable Island: ice and sea fluctuations from seismic stratigraphy on Sable Island Bank, Scotian Shelf, offshore Nova Scotia. *In* *Current Research, part D. Geological Survey of Canada Paper*, 2001-D19, 18p.
- Louden, K.E. 1994. The collection and analysis of seismo-acoustic data: results from Dalhousie ocean bottom seismograph recordings during CFAV QUEST cruise 211. Contractor Report: Defence Research Establishment Atlantic DREA CR/94/416, 45p.
- Moran, K., Piper, D., Mayer, L., Courtney, R., Driscoll, A., Hall, F. 1989. Scientific results of long coring on the eastern Canadian continental margin. *In* *Proceedings from the 21st Annual Offshore Technology Conference*, OTC 5963: 65-71.
- Moran, K., Courtney, R., Mayer, L., Miller, A., Zeuvenhuizen, J. 1991. Scotian shelf surficial geology and physical properties 12: central shelf: Emerald Basin. *In* *East Coast Basin Atlas Series: Scotian Shelf*; Atlantic Geoscience Center, Geological Survey of Canada, p 133.
- Osler, J. and Chapman, D. 1996. Seismo-acoustic determination of the shear-wave speed of surficial clay and silt sediments on the Scotian Shelf. *Defence Research Establishment Atlantic*, 12p.
- Piper, David. 1991. Surficial geology and physical properties 7: paleo-oceanography and paleo- glaciology. *In* *East Coast Basin Atlas Series: Scotian Shelf*; Atlantic Geoscience Center, Geological Survey of Canada, p123.

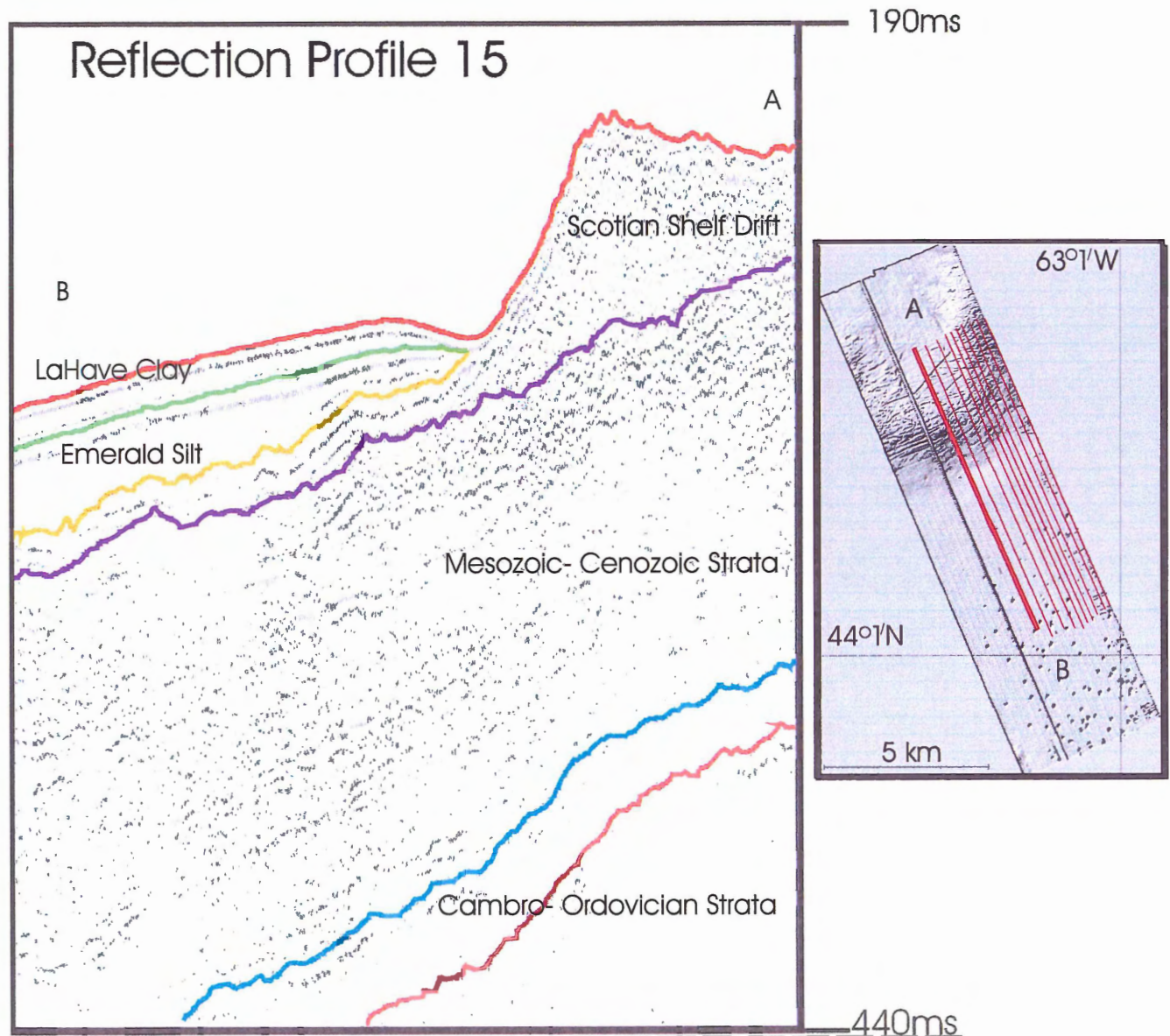
- Quinlan, G. and Beaumont, C. 1982. The deglaciation of Atlantic Canada as reconstructed from the postglacial relative sea-level record. *Canadian Journal of Earth Sciences*, **19**: 2232-2246.
- Stanford, B.J., Fader, G., and Moir, P. 1991. Scotian shelf regional geology and geophysics 8: bedrock geology. *In* East Coast Basin Atlas Series: Scotian Shelf; Atlantic Geoscience Center, Geological Survey of Canada, p23.
- Stea, R., Piper, D., Fader, G., Boyd, R. 1998. Wisconsinan glacial and sea-level history of Maritime Canada and the adjacent continental shelf: A correlation of land and sea events. *Geological Society of America Bulletin*, **110**: 821-845.
- Stea, R., Boyd, R., Fader, G., Courtney, R., Scott, D., Pecore, S. 1994. Morphology and seismic stratigraphy of the inner continental shelf off Nova Scotia, Canada: Evidence for a -65m lowstand between 11,650 and 11,250 C¹⁴ yr B.P. *Marine Geology*, **117**: 135-154.
- Vilks, G. and Rashid, M. 1976. Post-glacial paleo-oceanography of Emerald Basin, Scotian Shelf. *Canadian Journal of Earth Sciences*, **13**: 1256-1267.
- Wade, J. and MacLean, B. 1990. The geology of the southeastern margin of Canada, chapter 5: Aspects of the geology of the Scotian Basin from recent seismic and well data; part 2. *In* Geology of the Continental Margin of Eastern Canada, Geological Survey of Canada; **2**: 31-85.
- Zelt, C.A and Smith, R.B. 1992. Seismic travelttime inversion for 2-D crustal velocity structure. *Geophysical Journal International*, **108**: 16-34.

www.baylor.edu/~grass

www.phys.ocen.dal.ca/~deping. 2000.

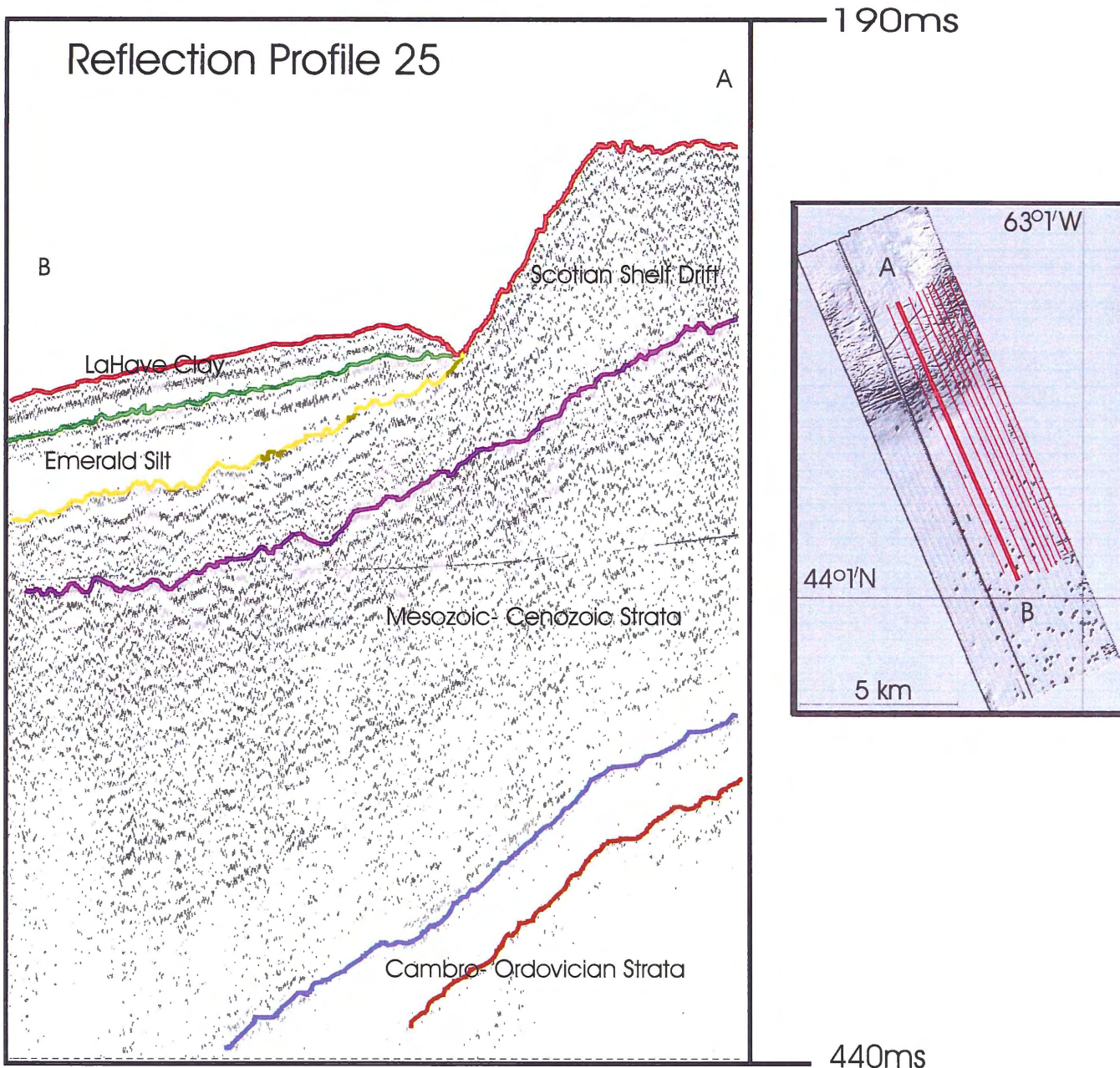
www.soest.hawaii.edu/gmt/gmt/doc/html

APPENDIX 1:
Horizons Digitized From Reflection Profiles



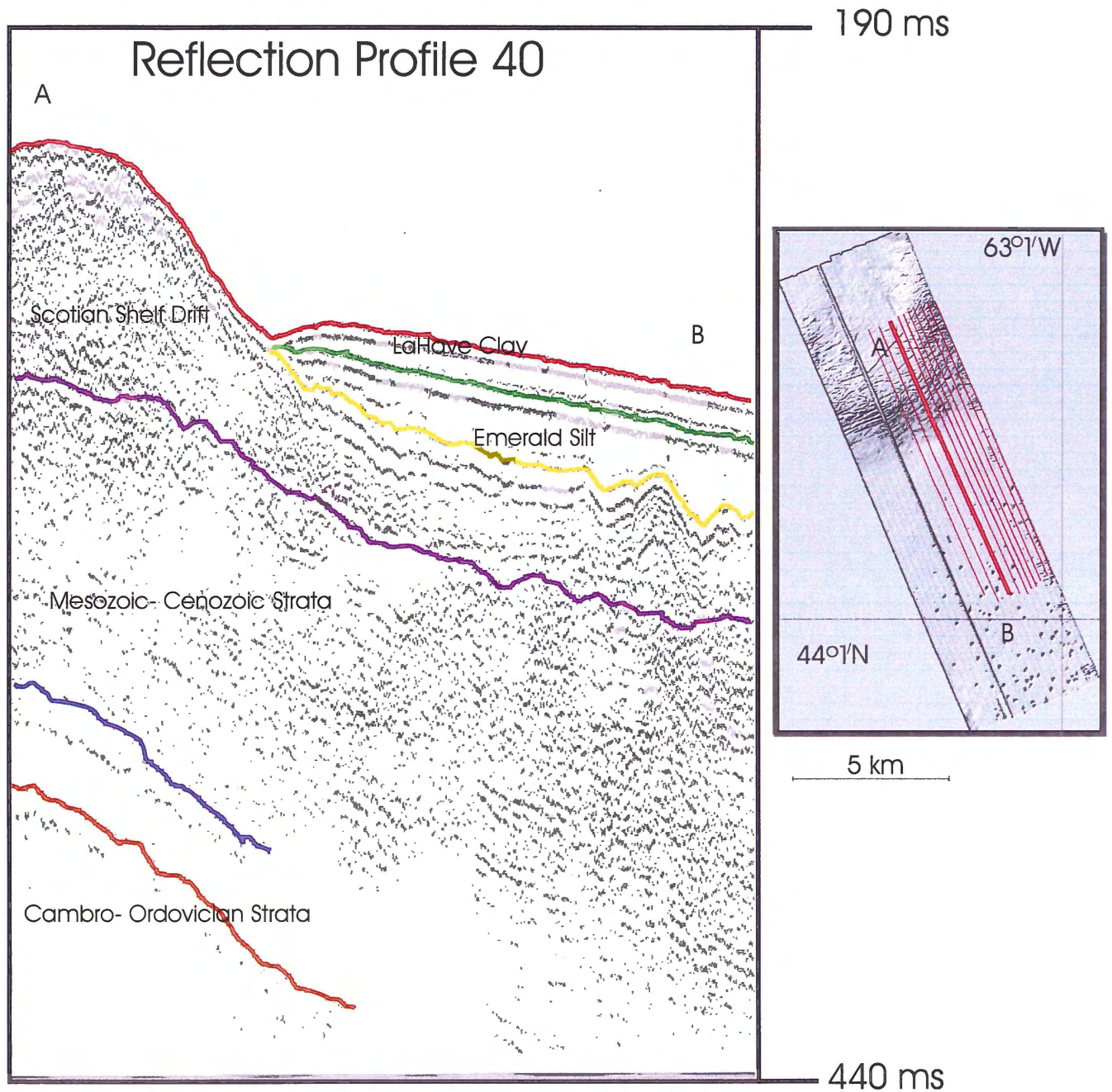
The image seen above represents a reflection profile recorded between 190 ms and 440 ms. The horizons that correspond with lithological units were digitized and are identified here in color. The red line represents the seafloor boundary, the green line traces the lower boundary of the LaHave Clay unit, the yellow line traces the lower boundary of the Emerald Silt unit, the purple line traces the lower boundary of the Scotian Shelf Drift unit, the blue line represents the lower boundary of the Mesozoic-Cenozoic Strata, which is also the upper boundary of the Cambro-Ordovician strata (basement), the orange line is another phase of the basement reflector.

The small map on the right shows the location of the profile with respect to the other 10 lines that were analyzed. Profile 15 is highlighted.



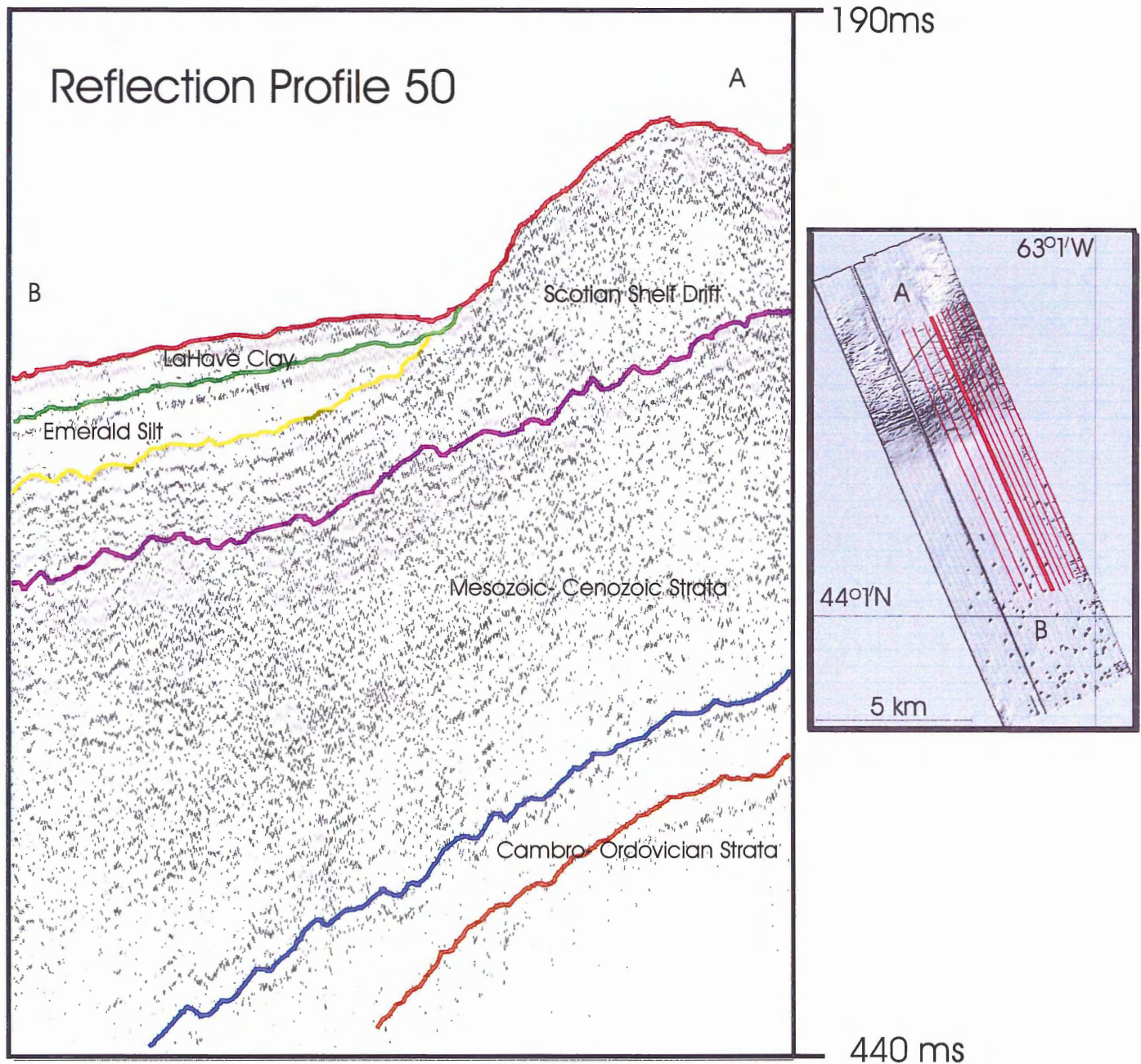
The image seen above represents a reflection profile recorded between 190 ms and 440 ms. The horizons that correspond with lithological units were digitized and are identified here in color. The red line represents the seafloor boundary, the green line traces the lower boundary of the LaHave Clay unit, the yellow line traces the lower boundary of the Emerald Silt unit, the purple line traces the lower boundary of the Scotian Shelf Drift unit, the blue line represents the lower boundary of the Mesozoic-Cenozoic Strata, which is also the upper boundary of the Cambro-Ordovician strata (basement), the orange line is another phase of the basement reflector.

The small map on the right shows the location of the profile with respect to the other 10 lines that were analyzed. Profile 25 is highlighted.



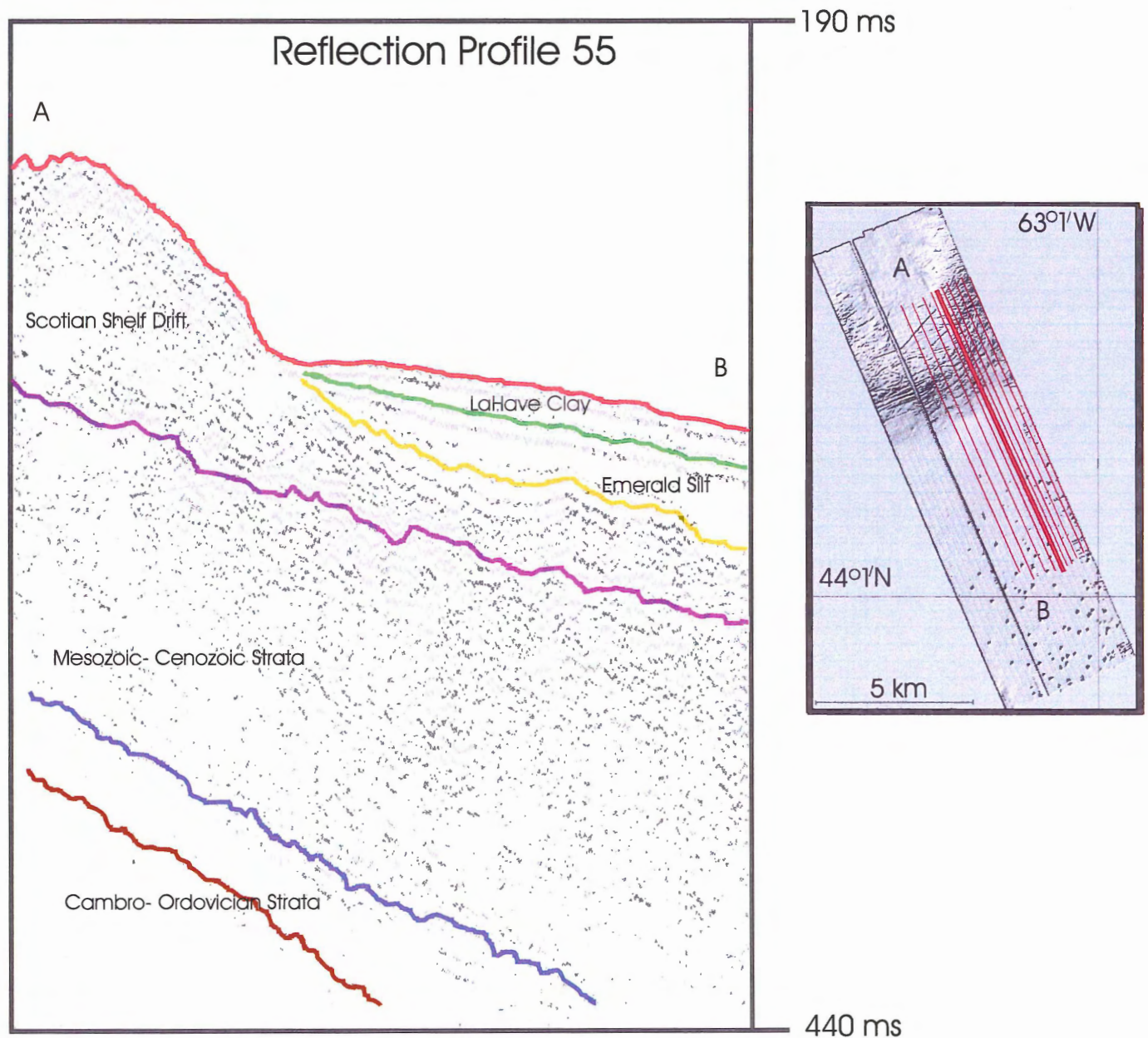
The image seen above represents a reflection profile recorded between 190 ms and 440 ms. The horizons that correspond with lithological units were digitized and are identified here in color. The red line represents the seafloor boundary, the green line traces the lower boundary of the LaHave Clay unit, the yellow line traces the lower boundary of the Emerald Silt unit, the purple line traces the lower boundary of the Scotian Shelf Drift unit, the blue line represents the lower boundary of the Mesozoic-Cenozoic Strata, which is also the upper boundary of the Cambro-Ordovician strata (basement), the orange line is another phase of the basement reflector.

The small map on the right shows the location of the profile with respect to the other 10 lines that were analyzed. Profile 40 is highlighted.



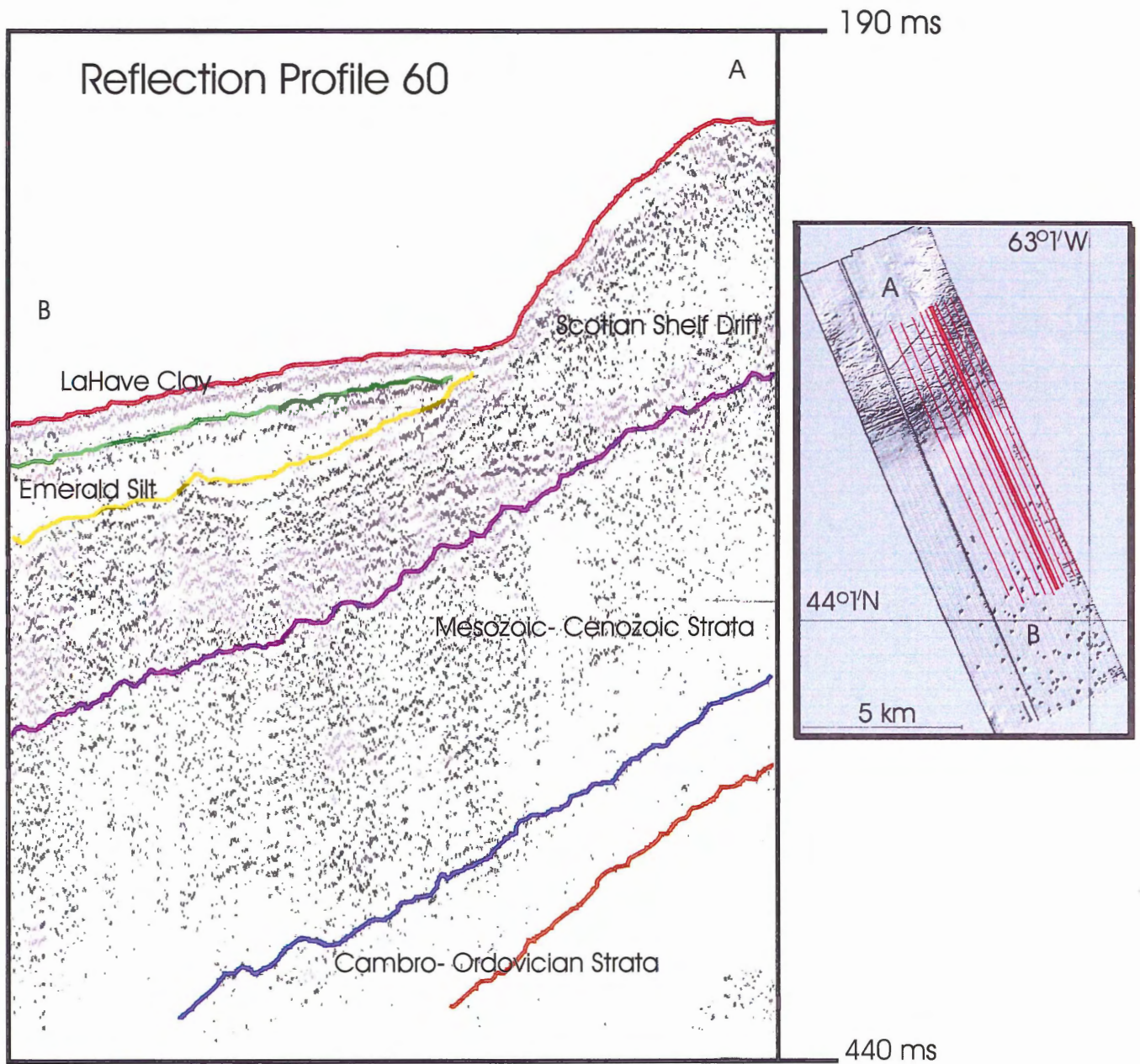
The image seen above represents a reflection profile recorded between 190 ms and 440 ms. The horizons that correspond with lithological units were digitized and are identified here in color. The red line represents the seafloor boundary, the green line traces the lower boundary of the LaHave Clay unit, the yellow line traces the lower boundary of the Emerald Silt unit, the purple line traces the lower boundary of the Scotian Shelf Drift unit, the blue line represents the lower boundary of the Mesozoic-Cenozoic Strata, which is also the upper boundary of the Cambro-Ordovician strata (basement), the orange line is another phase of the basement reflector.

The small map on the right shows the location of the profile with respect to the other 10 lines that were analyzed. Profile 50 is highlighted.



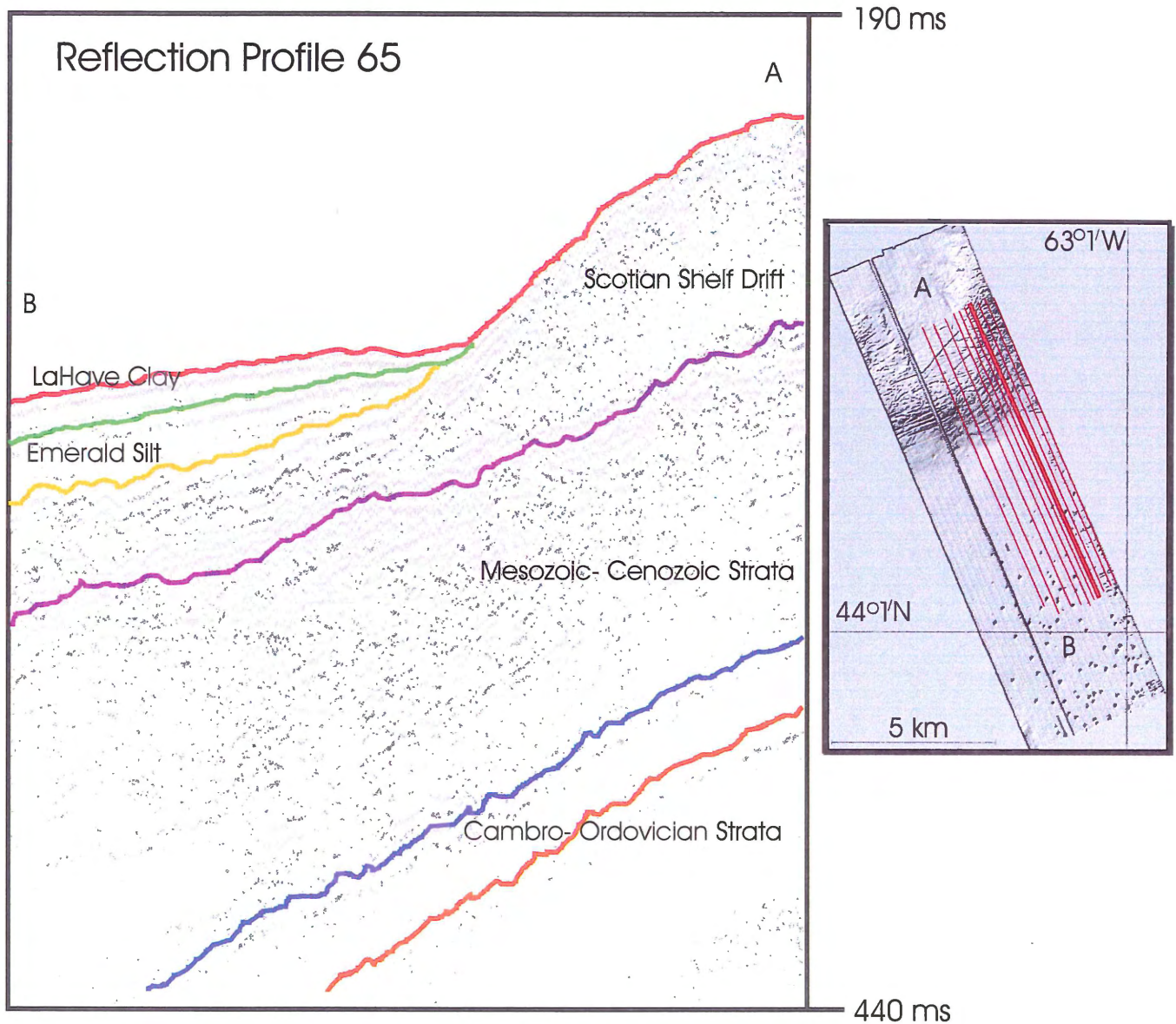
The image seen above represents a reflection profile recorded between 190 ms and 440 ms. The horizons that correspond with lithological units were digitized and are identified here in color. The red line represents the seafloor boundary, the green line traces the lower boundary of the LaHave Clay unit, the yellow line traces the lower boundary of the Emerald Silt unit, the purple line traces the lower boundary of the Scotian Shelf Drift unit, the blue line represents the lower boundary of the Mesozoic-Cenozoic Strata, which is also the upper boundary of the Cambro-Ordovician strata (basement), the orange line is another phase of the basement reflector.

The small map on the right shows the location of the profile with respect to the other 10 lines that were analyzed. Profile 55 is highlighted.



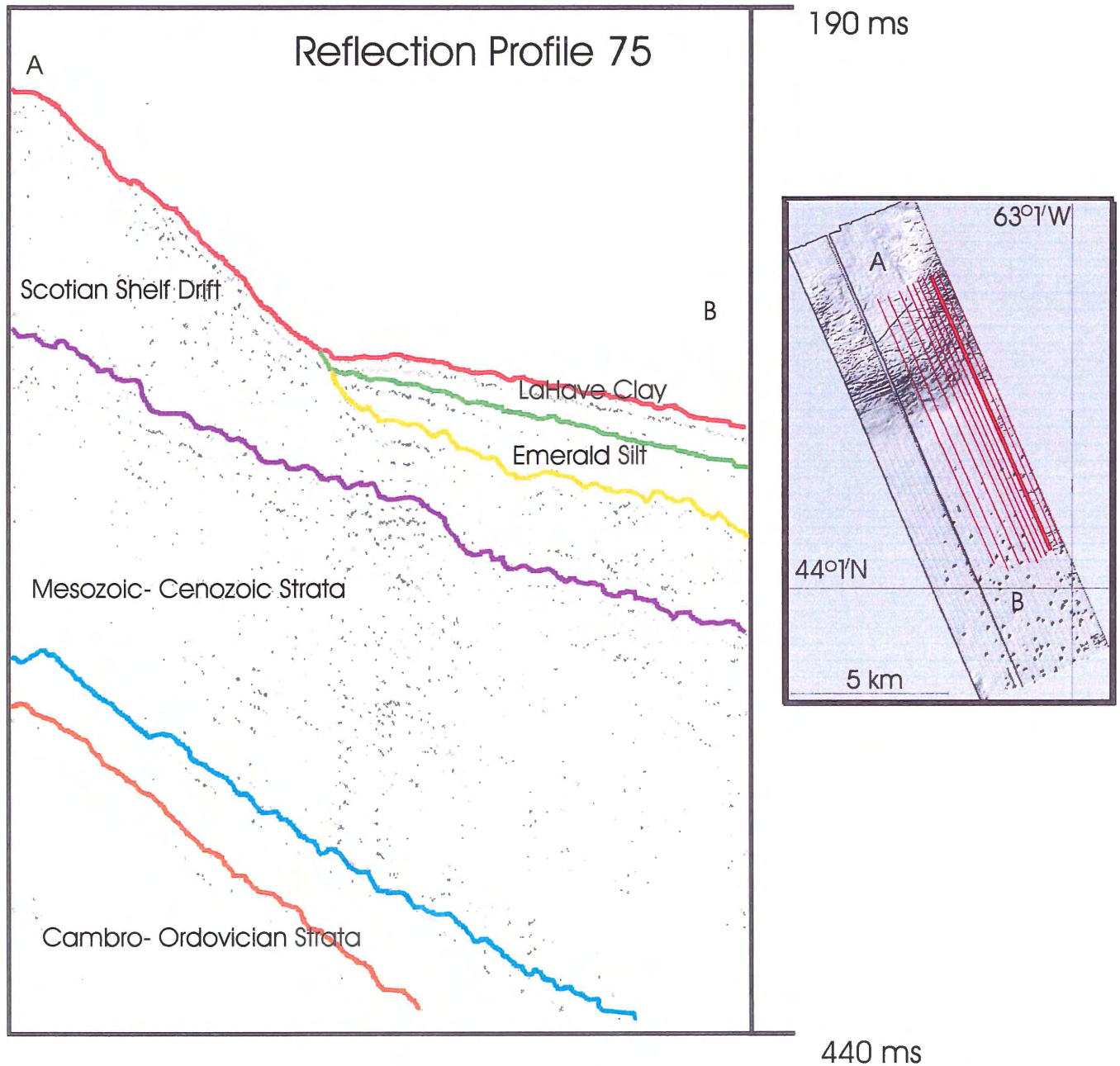
The image seen above represents a reflection profile recorded between 190 ms and 440 ms. The horizons that correspond with lithological units were digitized and are identified here in color. The red line represents the seafloor boundary, the green line traces the lower boundary of the LaHave Clay unit, the yellow line traces the lower boundary of the Emerald Silt unit, the purple line traces the lower boundary of the Scotian Shelf Drift unit, the blue line represents the lower boundary of the Mesozoic-Cenozoic Strata, which is also the upper boundary of the Cambro-Ordovician strata (basement), the orange line is another phase of the basement reflector.

The small map on the right shows the location of the profile with respect to the other 10 lines that were analyzed. Profile 60 is highlighted.



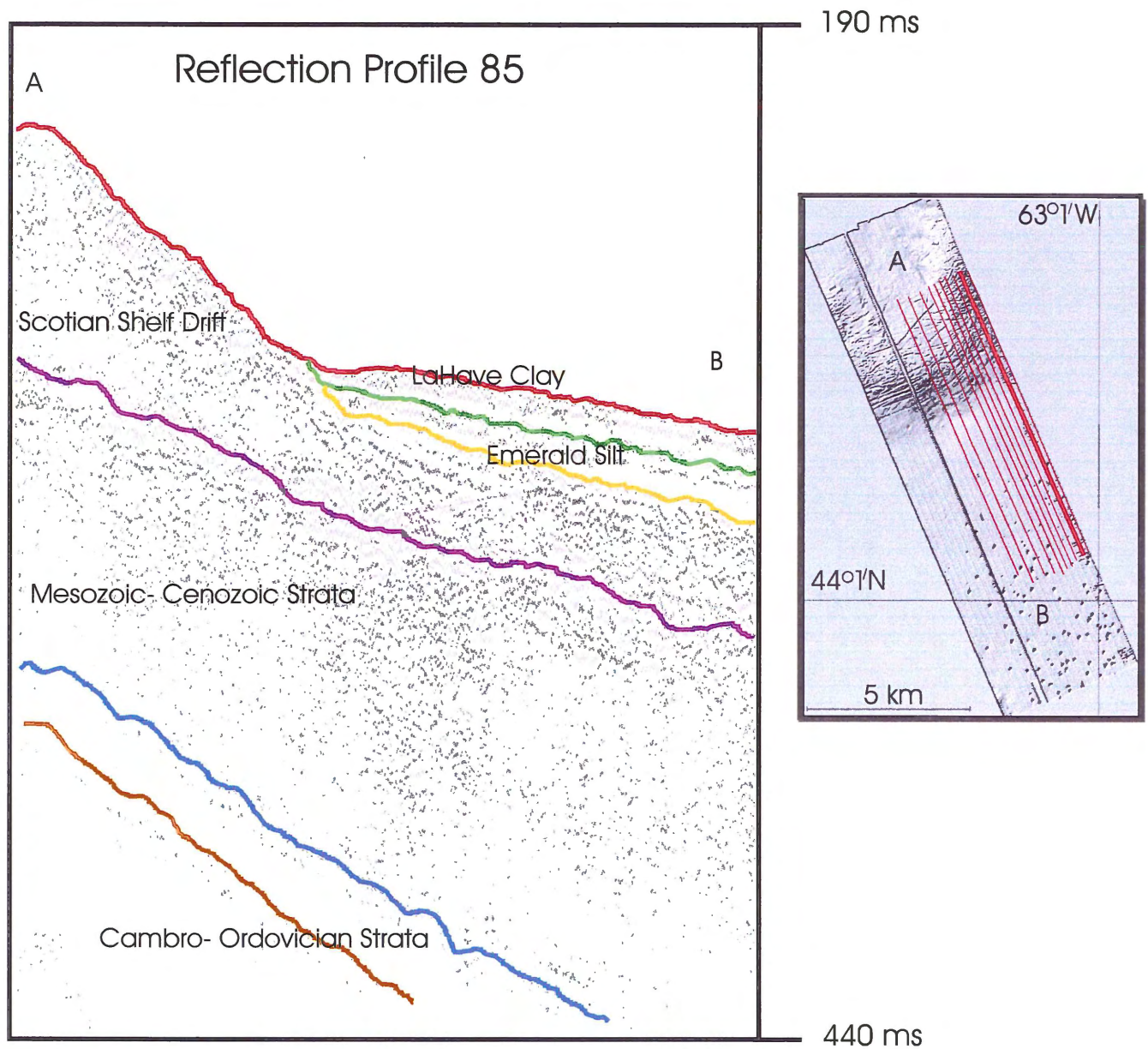
The image seen above represents a reflection profile recorded between 190 ms and 440 ms. The horizons that correspond with lithological units were digitized and are identified here in color. The red line represents the seafloor boundary, the green line traces the lower boundary of the LaHave Clay unit, the yellow line traces the lower boundary of the Emerald Silt unit, the purple line traces the lower boundary of the Scotian Shelf Drift unit, the blue line represents the lower boundary of the Mesozoic-Cenozoic Strata, which is also the upper boundary of the Cambro-Ordovician strata (basement), the orange line is another phase of the basement reflector.

The small map on the right shows the location of the profile with respect to the other 10 lines that were analyzed. Profile 65 is highlighted.



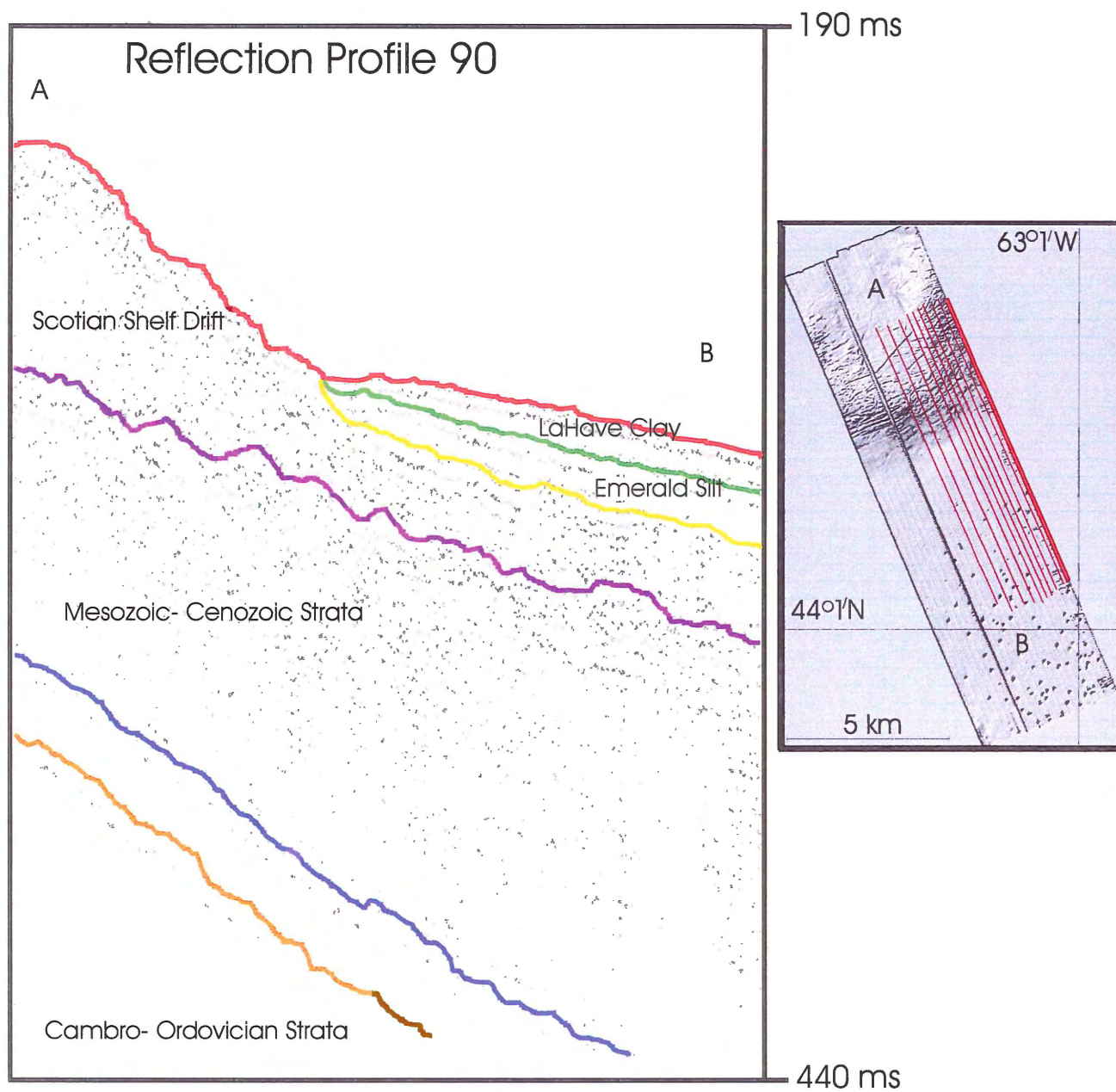
The image seen above represents a reflection profile recorded between 190 ms and 440 ms. The horizons that correspond with lithological units were digitized and are identified here in color. The red line represents the seafloor boundary, the green line traces the lower boundary of the LaHave Clay unit, the yellow line traces the lower boundary of the Emerald Silt unit, the purple line traces the lower boundary of the Scotian Shelf Drift unit, the blue line represents the lower boundary of the Mesozoic-Cenozoic Strata, which is also the upper boundary of the Cambro-Ordovician strata (basement), the orange line is another phase of the basement reflector.

The small map on the right shows the location of the profile with respect to the other 10 lines that were analyzed. Profile 75 is highlighted.



The image seen above represents a reflection profile recorded between 190 ms and 440 ms. The horizons that correspond with lithological units were digitized and are identified here in color. The red line represents the seafloor boundary, the green line traces the lower boundary of the LaHave Clay unit, the yellow line traces the lower boundary of the Emerald Silt unit, the purple line traces the lower boundary of the Scotian Shelf Drift unit, the blue line represents the lower boundary of the Mesozoic-Cenozoic Strata, which is also the upper boundary of the Cambro-Ordovician strata (basement), the orange line is another phase of the basement reflector.

The small map on the right shows the location of the profile with respect to the other 10 lines that were analyzed. Profile 85 is highlighted.



The image seen above represents a reflection profile recorded between 190 ms and 440 ms. The horizons that correspond with lithological units were digitized and are identified here in color. The red line represents the seafloor boundary, the green line traces the lower boundary of the LaHave Clay unit, the yellow line traces the lower boundary of the Emerald Silt unit, the purple line traces the lower boundary of the Scotian Shelf Drift unit, the blue line represents the lower boundary of the Mesozoic-Cenozoic Strata, which is also the upper boundary of the Cambro-Ordovician strata (basement), the orange line is another phase of the basement reflector.

The small map on the right shows the location of the profile with respect to the other 10 lines that were analyzed. Profile 90 is highlighted.